行政院國家科學委員會專題研究計畫 成果報告

可降解性Gellan gum做為新型生醫材料之可行性評估(第3年)
研究成果報告(完整版)

計 畫 類 別 ：個別型
計 畫 編 號 ：NSC 98-2221-E-040-007-MY3
執 行 期 間 ：100年08月01日至101年07月31日
執 行 單 位 ：中山醫學大學醫學檢驗暨生物技術學系（所）

計 畫 主 持 人：李明偉
共 同 主 持 人：張淑真

報 告 附 件 ：出席國際會議研究心得報告及發表論文

公 開 資 訊 ：本計畫涉及專利或其他智慧財產權，2年後可公開查詢

中 華 民 國 101年10月30日

中 文 摘 要 ： 結蘭膠(GG)是由 Sphingomonas elodea 所產生的胞外多醣體，為了發展出具有醫療應用性的結蘭膠，在此研究中準備了 26μm 厚的結蘭膠膜和 1-乙基-3-碳化二亞胺(EDC)反應於 40%的乙醇中，而得到交聯膜(GG40)(含有 73%的膠和 52.4 MPa 的張力強度)。在體外的生物相容性試驗中，GG40 膜對於 L929 細胞顯現出無毒反應，但會抑制血小板的吸收及活性。當將 GG40 膜植入老鼠的皮下組織時，在早期的術後時期會造成較小的發炎反應。結果顯示 GG40 膜對傷口癒合、傷口大小的復原(%)和膠原的含量都較其它商品(人工皮)來的好，因此，作者推斷結蘭膜在此研究中的發展對於未來用於外科手術應用上是有它的潛力的。

中文關鍵詞： 結冷膠,傷口敷料,EDC

英 文 摘 要 ： Gellan gum (GG) is an exopolysaccharide produced by Sphingomonas elodea. To develop a medical application for GG, in this study we prepared 26 m thick films of GG reacted with 1-ethyl-3-(3-dimethylaminopropyl)carbodiimide (EDC) in 40% ethanol to obtain a cross-linked film (GG40) with 73% gel content and 52.4MPa tensile strength. In vitro biocompatibility tests, GG40 film exhibit nontoxic effects for L929 cells and inhibit absorption and activation of platelets. When implanted into rat subcutaneous
tissue, the GG40 film caused minor inflammation in the early postoperative period. The results indicate that the effects of GG40 film on wound healing, wound size reduction (%) and collagen content are higher than those found in commercial products (Duoderm). Therefore, we conclude that the GG film developed in this study has potential for future use in surgical applications.

英文關鍵詞： gellan gum, wound dressing, EDC

行政院國家科學委員會補助專題研究計畫
成果報告

可降解性 Gellan gum 做為新型生醫材料之可行性評估

計畫類別：■個別型計畫　□整合型計畫

計畫編號：NSC　98－2221－E　－040　－007－MY3

執行期間：98 年 8 月 1　日至 101 年 7 月 31　日

執行機構及系所：中山醫學大學醫學檢驗暨生物技術學系

計畫主持人：李明偉

共同主持人：張淑真

計畫參與人員：黃佳慧、吳雅蓉、阮筠珍、黃怡婷、溫淑敏、尤振霖、陳翊民

成果報告類型(依經費核定清單規定繳交)：□精簡報告　■完整報告

處理方式：除列管計畫及下列情形者外，得立即公開查詢

■涉及專利或其他智慧財產權，□一年□二年後可公開查詢

中　華　民　國 101 年 10　月 30　日

本 3 年期研究計畫執行期間共發表 8 篇 SCI 期刊，結案報告的撰寫方式則是依據發表期刊的主題，分述其詳細內容，結果呈現如下：

研究主題一：Use of gellan gum to decrease postoperative adhesions in a rat model—physical and biological effects

Abstract

A new anti-adhesion membrane made from gellan gum was fabricated and characterized. We prepared a 12 μm-thick membrane of gellan gum and reacted it with 1-ethyl-3-(3-dimethylaminopropyl) carbodiimide in 70% acetone to obtain a cross-linked membrane (G/A70) with 87% gel content and a 46.5 MPa tensile strength. In vivo evaluation of postoperative tissue adhesion showed that the use of a G/A70 membrane reduced the adhesion incidence by 90%. We used real-time quantitative RT-PCR to analyze inflammation-related and extracellular matrix protein gene expression in a rat model of abdominal surgery. On day 3 after surgery, the gene expression of ceruloplasmin and type V collagen in the G/A70-treated group was 1.9 and 0.3 times that of the control group, respectively. The results indicated that G/A70 elicited mild inflammation but could suppress type V collagen synthesis and reduce the occurrence of tissue adhesion. These findings may provide insights into the properties of the gellan gum anti-adhesion membrane and might also help to overcome problems involving tissue adhesions in surgical procedures.

1. Introduction

Postsurgical abdominal adhesions are one of the most urgent problems in surgery today. The incidence of intra-abdominal adhesions ranges from 67 to 93% after general abdominal surgical procedures and can cause intestinal obstruction (74%), chronic pelvic pain (20-50%), and female infertility (15-20%) [1]. Intra-abdominal adhesion formation is the result of both insufficient fibrinolytic capacity and increased fibrin formation in response to the enhanced inflammatory state of the peritoneum. Normal fibrinolytic activity prevents fibrinous attachments after surgery, and mesothelial repair occurs within 5 days of trauma. During this period, a single cell layer of new peritoneum covers the injured area, replacing fibrinous exudates. However, if fibrinous activity is suppressed, fibroblasts will migrate, proliferate and form adhesions. Collagen is deposited, and neovascular formation starts [2].

One of the most commonly used anti-adhesion devices is a polymeric membrane that separates and isolates the wounded tissue after surgery. Currently, several products are used for reducing tissue adhesion, but none of them are completely satisfactory in clinical practice. In this study, we aimed to develop an anti-adhesion

membrane based on gellan gum because of its biocompatibility and low cytotoxicity [3]. Gellan gum is a microbial polysaccharide that is produced by fermentation. The microorganism naturally responsible for this fermentation is *Sphingomonas elodea*, which lives on an aquatic plant, *Elodea canadensis*. Gellan gum, also called polysaccharide ps-60, was discovered in 1978 and rapidly received USFDA approval in 1992 for use in food and drinks [4]. Recently, gellan gum has been investigated as a candidate biomaterial for tissue engineering, guided bone regeneration [5], drug-carrier matrices [6], gene delivery agents [7] and cell-carrier materials [8-9]. Previously, we fabricated a photo-cross-linked gellan gum membrane and showed that it had significant potential for the prevention of postoperative adhesions [10]. Here, we prepared a gellan gum membrane by using 1-ethyl-3-(3-dimethylaminopropyl) carbodiimide (EDC) as the cross-linking agent and investigated the chemical and physical properties of the membrane. In addition, to analyze the molecular mechanism for the gellan gum anti-adhesion effect in more detail, we tracked inflammation-related (ceruloplasmin) and extracellular matrix protein (type V collagen) gene expression in a rat model of abdominal surgery.

2. Materials and Methods

2.1. Preparation of the gellan gum membrane

To prepare the membrane, 0.3 g of gellan gum (GG) (Sigma G1910) was dissolved in 30 ml of deionized water (DDW) and heated at 85–90 ℃ until it became a transparent solution. The solution was then poured onto a glass dish (diameter 10 cm) and evaporated at 37 ℃ and 1 atm for 3 days to obtain a dry gellan gum membrane. The gellan gum membranes were then cross-linked by immersing them into an acetone/DDW solution containing 15 mM 1-ethyl-3-(3-dimethylaminopropyl) carbodiimide (EDC, sigma 1769) for 24 h at room temperature. To study the effects of acetone composition on the EDC cross-linking of the gellan gum, acetone was mixed with DDW to yield varying acetone/DDW (v/v%) solutions. This study used 0%, 30%, 50%, 70% and 90% acetone/DDW solutions. The cross-linked membranes (denoted as G/A0, G/A30, G/A50, G/A70 and G/A90) were washed with 95% ethanol three times to remove any nonreacted residual EDC and then dried at room temperature [11].

2.2. Characterization of the gellan gum membranes

We used an FTIR-L396A (Perkin-Elmer) to analyze the properties of the chemical functional groups of the gellan gum membranes. Analysis of the gel content of the gellan gum membranes was performed as follows: After drying, the cross-linked membrane (W_1) was weighed, and then it swelled in DDW at 37 ℃ for 24 h. After the

wet membrane was removed from the solution, it was dried in a vacuum oven for 12 h at 60 °C and then weighed again (W_2). The following equation was then used to calculate the gel content of the membrane [12]: gel content (%) = (W_2/W_1) x 100.

2.3. Mechanical property measurement

Gellan gum membranes were cut into 1 cm × 5 cm pieces (Kuo et al., 2009). We then used the H1-KS testing machine (Tinius Olsen) with a crosshead speed of 5 mm/min to measure the mechanical properties of the gellan gum membranes and to automatically record the mechanical parameters [10].

2.4. Animal implant study

Twenty Sprague-Dawley rats (200–250 g) were tested in a surgical research laboratory. Aseptic midline laparotomies were conducted while the animals were anesthetized with 4% trichloroacetaldehyde monohydrate (1 ml/100 g). The distal 3 cm of the cecum and the opposing abdominal wall were scraped with a scalpel until the serosal surface was disrupted and hemorrhaged but not perforated. The denuded peritoneal wall was then covered with a gellan gum membrane (diameter: 1.0 cm). The rats in the control group were not covered with any anti-adhesion membrane. Contact between the cecum and opposing peritoneal wall was maintained in all animal groups with two nonoccluding loops of 4/0 polypropylene suture placed 2 cm apart. After the completion of the procedure, the abdomen was closed in a double layer using 4/0 polypropylene in a continuous fashion. The experimental rats were sacrificed on day 3 or 7 after surgery to examine the process of adhesion formation at the injury site. The abdominal wall of the injury site was removed and fixed in a 10% formalin solution. The tissues were processed by the standard procedure for histological examinations, and thin sections were examined after staining with hematoxylin-eosin (H&E stain) [11].

2.5. Real-Time Quantitative Reverse Transcription Polymerase Chain Reaction (qRT-PCR)

The total RNA was extracted from the abdominal wall of the injured site using a FavorPrep™ Tissue Total RNA Mini Kit according to the manufacturer's protocol. A total of 5 μg of total RNA was used to synthesize cDNA using a SuperScript™ III First-Strand Synthesis System (Invitrogen) according to the manufacturer instructions. The cDNA was amplified using SYBR green PCR reagents, and the qRT-PCR reactions were conducted using the StepOne™ Real-Time PCR System (Applied Biosystems). The following primer sequences were used:

Ceruloplasmin [13], 5'- ATTACATCGCTGCCGAGGAGA-3' (forward)

5’- GGAGGCTTGCTTTGAGGAACG-3’ (reverse)

Type V collagen [14], 5’-CCATCAATGACCAACACAAG-3’ (forward)

5’- GGTCAGGCACTTCAGATCAT-3’ (reverse)

β-actin, 5’-TGATGATATCGCCGCGCTCGTCGT-3’ (forward)

5’-CACAGCCTGGATAGCAACGTACAT-3’(reverse).

β-actin was used as a housekeeping gene. All reactions were performed in duplicate, followed by a melting-curve analysis for each qRT-PCR run. The expression levels were calculated using the comparative CT method.

2.6. Statistical analysis

Each of the experiments was repeated at least four times, and the values were expressed as the means ± standard deviations. For a comparison between the two groups of data, Student’s *t*-test was performed. Differences were considered to be statistically significant at $P < 0.05$.

3. Results

3.1. Gel content of the cross-linked gellan gum membrane

EDC is the most widely used reagent for chemical cross-linking. To solve the problem of EDC hydrolysis in water [15-16], this study used a mixture of acetone/DDW as the reaction solvent. Fig. 1 shows the gel content of gellan gum membranes cross-linked in various concentrations of acetone with 15 mM EDC for 24 h. In the control group (without acetone), the gel content of the gellan gum membrane was found to be only 21±4.3%, and it showed a low degree of cross-linking. In 70% acetone (G/A70 membrane), the gel content was found to be the highest (87±7.2%). An acetone content of 70% was found to be the most suitable condition for the cross-linked gellan gum.

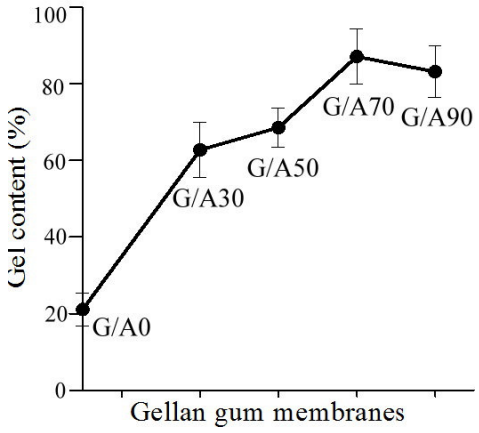

Fig. 1. The gel content of gellan gum membranes cross-linked in various concentrations of acetone with 15 mM EDC for 24 h.

3.2. Mechanical properties of the gellan gum membrane

Fig. 2 shows the tensile strength of the gellan gum membranes cross-linked in various concentrations of acetone with 15 mM EDC for 24 h. The average thickness of the membranes was 12.6 μm. The results indicate that G/A30, G/A50, G/A70 and G/A90 have high tensile strengths of 37.9±4.4, 40.5±4.0, 46.5±3.4 and 45.9±8.4 MPa, respectively. Previous studies demonstrate that the tensile strength of a polymer is closely correlated to the density of cross-linking [17]. At a lower cross-link density, the tensile strength increases with an increase in the cross-link density. Based on the gel content and mechanical property measurements, creating gellan gum membranes in 70% acetone optimizes the cross-linked environment. Therefore, in this study, we selected the G/A70 gellan gum membrane as the substrate of choice for evaluating the effects of the gel on tissue anti-adhesion.

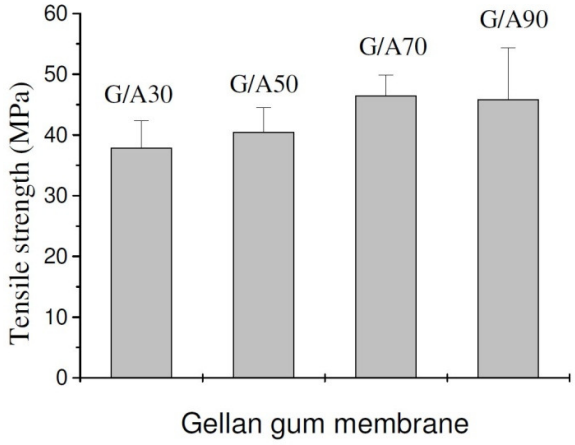

Fig. 2. The tensile strength of gellan gum membranes cross-linked in various concentrations of acetone with 15 mM EDC for 24 h.

3.3. FTIR characterization of the gellan gum membrane

FTIR was used to analyze the structure of non-cross-linked and cross-linked (G/A70) membranes. The FTIR spectrum (Fig. 3) shows the assignment of the absorption band at 3318 cm^{-1} to the stretching of the -OH groups in the gellan gum [3,18]. The band at 2923 cm^{-1} is due to the stretching vibrations of the -CH_2 group, whereas the bands appearing at 1149 and 1022 cm^{-1} are due to ethereal and hydroxylic C-O stretching. The peaks at 1604 and 1404 cm^{-1} can be assigned to the characteristic absorption band of carboxyl groups in the gellan gum. The bending vibration of C-H appears at 836 cm^{-1}. For the FTIR spectrogram of the G/A70 membrane, the most prominent difference in the spectrum between non-cross-linked and cross-linked gellan gum appeared as a new absorption peak at 1726 cm^{-1}, which was assigned to the C=O ester group. This result indicates that the carboxyl group on

the β-D-glucuronic acid (Glcp A) in gellan gum can generate an ester bond with the -OH groups. The carboxyl group also causes the absorption peak of the -OH groups to shift to a higher wave number (3325 cm^{-1}), however, the absorption peak of the –CH2 groups (836 cm^{-1}) shows no shift either before or after cross-linking.

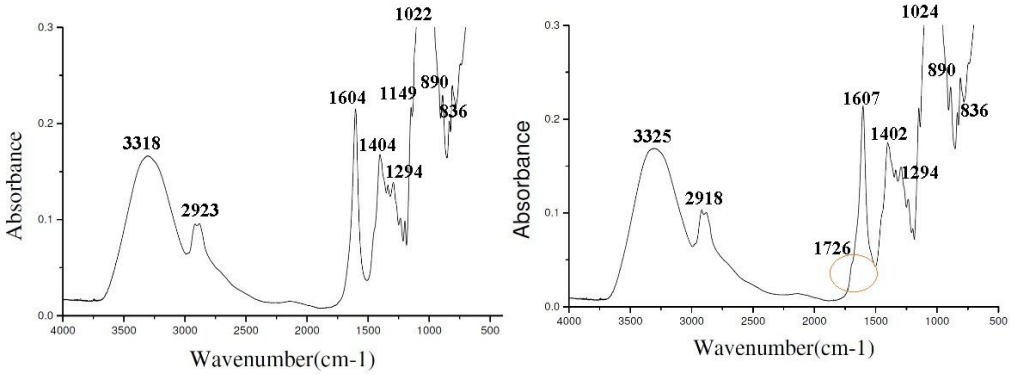

Fig. 3. FTIR spectra of non-cross-linked (left) and cross-linked (right) gellan gum membranes.

3.4. Animal implant study

The G/A70 membrane was tested as a physical barrier to prevent tissue adhesion following abdominal surgery. The occurrence of tissue adhesion between the cecum and the peritoneum was examined on the 3rd and 7th day after surgery. In the control group (without a membrane), severe tissue adhesions (Figs. 4a and 4b) of the cecum to the peritoneal wall were found in 8 of the 10 rats that received the operation. The G/A70 membrane, however, effectively prevented tissue adhesion in almost all (9 out of 10) rats operated on, i.e., the injured sites recovered without any tissue adhesion (Figs. 4c and 4d). The superior anti-adhesion capability of the G/A70 membrane was demonstrated throughout the observation period, and the statistics for the tissue adhesion in the two test groups are summarized in Table 1.

Table 1. Formation of postsurgical tissue adhesions in the rats after operation.

	3 days	7 days	Combined data
control	3/5[a]	5/5	8/10
G/A70 membrane	0/5	1/5	1/10

[a]Number of rats that formed tissue adhesions/number of rats receiving the operation

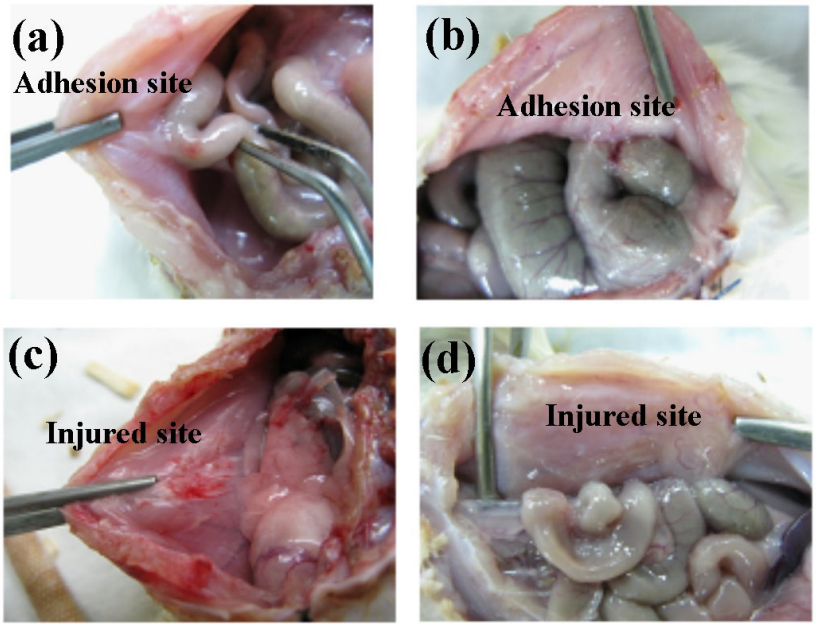

Fig. 4. Repair of the injured sites between the cecum and the peritoneal wall in the operated rats 3 and 7 days after surgery : (a, b) adhesion formation (control group) and (c, d) treated with the G/A70 membrane without adhesion formation.

The tissues surrounding the injury sites of the rats were dissected and examined. Photomicrographs of the sectioned, H&E-stained tissues on day 3 and day 7 of the repair process are shown in Figs. 5a and 5b. In the control group, newly formed adhesive tissue was found between the peritoneal wall and the mucosa of the cecum [15]. In the experimental group, on day 3 after surgery, the surgical lesions had not completely healed and did not form adhesive tissue between the peritoneal wall and the mucosa of the cecum (Fig. 5c). On day 7 after surgery (Fig. 5d), the tissues around the surgical lesions had completely healed. Histologically, on days 3 and 7 following surgery, the inflammatory cells were prominent near the surgical lesions, indicating that the G/A70 membrane caused acute inflammation—a normal tissue reaction immediately after implantation.

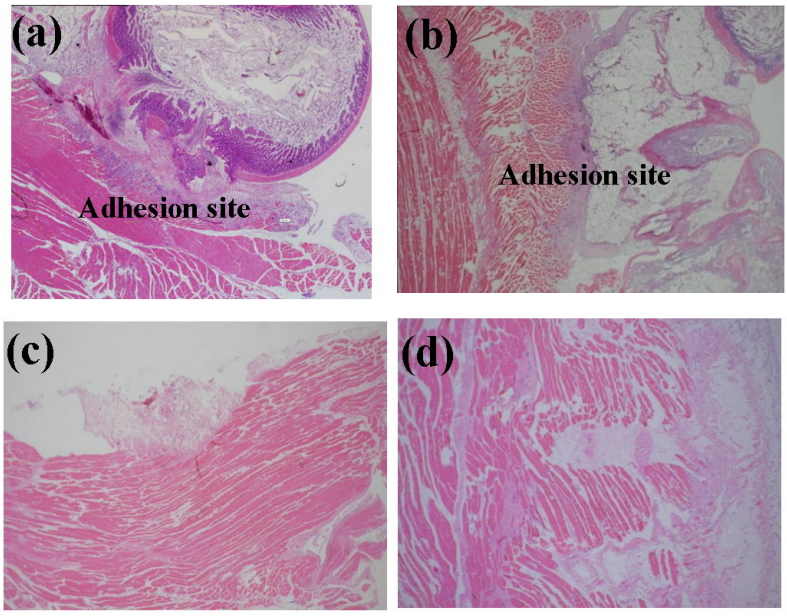

Fig. 5. Histological observation of the wound site in the rats 3 and 7 days after surgery：(a, b) control group and (c, d) treated with the G/A70 membrane. These sections were stained with H&E (100x).

3.5. Ceruloplasmin and type V collagen gene expression

It was noted that the G/A70 membrane exhibited a promising anti-adhesion potential. To analyze the molecular mechanism for the gellan gum anti-adhesion effect in more detail, we tracked inflammation-related (ceruloplasmin) and extracellular matrix protein (type V collagen) gene expression in a rat model of abdominal surgery. Ceruloplasmin (Cp), a copper protein with important functions in inflammation, is usually used as a marker of inflammation at the acute injury stage. Fig. 6 shows the gene expression of ceruloplasmin determined by qRT-PCR. On day 3 and day 7 after surgery, the gene expression of ceruloplasmin in the G/A70 experimental group was 1.9 and 1.3 times that of the control group. These results indicate that G/A70 could elicit mild inflammation but not affect the anti-adhesion efficacy. Type V collagen is the most advanced essential agent for adhesive tissue formation. Gene expression of type v collagen determined by qRT-PCR is shown in Fig 7. On day 3 and day 7 after surgery, the gene expression of type V collagen in the G/A70 experimental group was 0.35 and 0.33 times that of the control group. The results indicate that G/A70 can suppress type V collagen synthesis and reduce the occurrence of tissue adhesion.

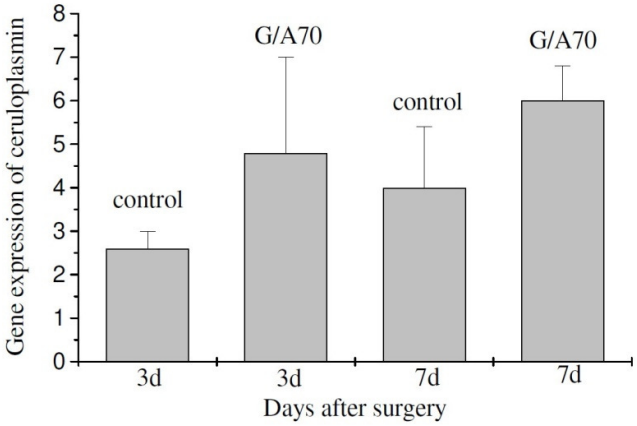

Fig. 6. Gene expression of ceruloplasmin on the 3rd and 7th days after surgery (n=5, results are given as the mean values, bars represent standard deviation).

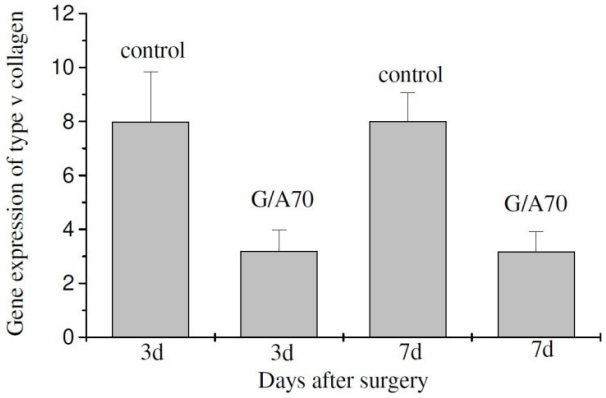

Fig. 7.Gene expression of type V collagen on the 3rd and 7th days after surgery (n=5, results are given as the mean values, bars represent standard deviation).

Discussion

EDC is the most widely used reagent for polysaccharide cross-linking in medical applications. To solve the problem of EDC hydrolysis in water, previous studies have suggested using a mixture of ethanol/DDW as the reaction solvent. In our previous work, it was found that an ethanol content of 40% was the most suitable condition for cross-linked gellan gum. In 40% ethanol, the physical properties of the EDC cross-linked gellan gum membrane showed the highest gel content (73%). In this study, we used acetone/DDW as the reaction solvent and studied the effects of the acetone composition on the EDC cross-linking of the gellan gum. The results indicated that the gel content of cross-linked gellan gum increased to 87% using 70% acetone as the reaction solvent. The gel content was increased due to a higher degree

of cross-linking as a result of the slower hydrolysis of EDC in 70% acetone compared with 40% ethanol. In addition, the increase in gel content was not proportional to the acetone content due to the difficulty of hydrophilic gellan gum polymer chain extension in organic solvents, which reduces its reactivity.

The tensile strength of a polymer is closely correlated to the density of cross-linking [19]. The mechanical testing results indicate that the G/A70 gellan gum membrane had the highest tensile strength of 46.5 MPa and that the increase in tensile strength was not proportional to the acetone content. The trend of gel content and tensile strength results are similar. At present, no standards regarding the mechanical properties of anti-adhesion membranes are available for clinical evaluation. In this study, the in vivo evaluation of the G/A70 gellan gum membrane for the prevention of postoperative adhesions showed that the membrane had sufficient mechanical strength and was easy to apply.

Many anti-adhesion products are based on anionic polysaccharides because of their negatively charged surface and good biocompatibility [20]. It is conceivable that the distinct cellular context could alter the expression of molecules on the cell surface and extracellular matrix, which in turn could alter the adhesion strength of a cell to a given biomaterial. In a previous study, Sung-Liang Yu [21] confirmed that ceruloplasmin expression increased the onset of inflammation following damage to the abdominal tissue. In this work, we tracked ceruloplasmin protein gene expression in a rat model of abdominal surgery and indicated that the gene expression of ceruloplasmin in the experimental group was higher than in the control group. Therefore, we confirmed that the G/A70 membrane could elicit mild inflammation. We speculate that this inflammation is due to the membrane disintegrating rapidly into small fragments and triggering fibroblast-secreted ceruloplasmin. Inflammation is a major stimuli for tissue adhesion [22-23], but here, G/A70-induced inflammation did not affect the anti-adhesion efficacy. Sung-Liang Yu et al. also demonstrated that the expression of collagen V concurred with the time-course of adhesion formation. Type V collagen, a component of the ECM that is located in a variety of tissues and capillary basement membranes, could play a role in angiogenesis [24-26]. Much of the previous work indicated that vascular endothelial growth factor (VEGF) and type V collagen expression increase during angiogenesis and are necessary for adhesion formation. In this work, we found that the gene expression of type V collagen in the G/A70-treated group was not increased at the time of adhesion formation. Moreover, type V collagen expression in the G/A70-treated group was lower than that of the control group 3 and 7 days after surgery. Therefore, we assumed that the molecular mechanism for the gellan gum anti-adhesion effect was via suppression of type V collagen synthesis and angiogenesis. In the future, we need to design molecular biology experiments to

confirm this hypothesis.

Conclusion

Gellan gum is a novel biodegradable material for preventing postsurgical adhesions. Here, we reported the optimization of the preparation process for gellan gum membranes and revealed the physical and biological effects of gellan gum on decreasing postoperative adhesions in a rat model. These findings may provide insights into the properties of the gellan gum anti-adhesion membrane and might also help to overcome this difficult problem involving tissue adhesions in surgical procedures.

Reference

[1]. Jean D, Revaz B, Sandrine P, Nicolas B, Kris J, Benoit R, Michel C, Gerard M. Incidence of intra-abdominal adhesions in a continuous series of 1000 laparoscopic procedures. Am J Obstet Gynecol 2010; 203(2): 111.e1-3.

[2]. Hellebrekers BWJ, Kooistra T. Pathogenesis of postoperative adhesion formation. Brit J Surg 2011; 98: 1503-1516.

[3]. Lee MW, Chen HJ, Tsao SW. Preparation, characterization and biological properties of Gellan gum films with 1-ethyl-3-(3-dimethylaminopropyl) carbodiimide cross-linker. Carbohyd Polym 2010; 82 (3): 920-926.

[4]. Rinaudo M, Milas M. Gellan gum, a bacterial gelling polymer. Dev Food Sci 2000; 41: 239-263.

[5]. Chang SJ, Kuo SM, Liu WT, Greory Niu CC, Lee MW, Wu CS. Gellan gum film for effective guided bone regeneration. J Med Biol Eng 2010; 30 (2): 99-103.

[6]. Ahuja M, Yadav M, Kumar S. Application of response surface methodology to formulation of ionotropically gelled gum cordia/gellan beads. Carbohyd Polym 2010; 80 (1): 161-167.

[7]. Goyal R, Tripathi SK, Tyagi S, Ram KR, Ansari KM, Kumar P, Shukla Y, Chowdhuri DK, Gupta KC. Gellan gum blended PEI nanocomposites as gene delivery agents: Evidences from in vitro and in vivo studies. Eur J Pharm Biopharm 2011; 79 (1): 3-14.

[8]. Wang C, Gong Y, Lin Y, Shen J, Wang DA. A novel gellan gel-based microcarrier for anchorage-dependent cell delivery. Acta Biomater 2008; 4(5): 1226-1234.

[9]. Silva NA, Cooke MJ, Tam RY, Sousa N, Salgado AJ, Reis RL, Shoichet MS. The effects of peptide modified gellan gum and olfactory ensheathing glia cells on neural stem/progenitor cell fate. Biomaterials 2012; 33 (27): 6345-6354.

[10]. Lee MW, Tsai HF, Wen SM, Huang CH. Photocrosslinkable gellan gum film as

an anti-adhesion barrier. Carbohyd Polym 2012; 90 (2): 1132-1138.
[11]. Lee MW, Hung CL, Cheng JC, Wang YJ. A new anti-adhesion film synthesized from polygalacturonic acid with 1-ethyl-3-(3-dimethylaminopropyl)carbodiimide crosslinker. Biomaterials 2005; 26 (18): 3793-3799.
[12]. Tomihata K, Ikada Y. Preparation of cross-linked hyaluronic acid films of low water content. Biomaterials 1997; 18 (3): 189-195.
[13]. Chang YZ, Qian ZM, Wang K, Zhu L, Yang XD, Du JR, Jiang L, Ho KP, Wang Q, Ke Y. Effects of development and iron status on ceruloplasmin expression in rat brain. J Cell Physiol 2005; 204(2): 623-631.
[14]. Zhang M, Pritchard MR, Middleton FA, Horton JA, Damron TA. Microarray analysis of perichondral and reserve growth plate zones identifies differential gene expressions and signal pathways. Bone 2008; 43: 511-520.
[15]. Nam K, Kimura T, Funamoto S, Kishida A. Preparation of a collagen/polymer hybrid gel designed for tissue membranes. Part I: controlling the polymer-collagen cross-linking process using an ethanol/water co-solvent. Acta Biomater 2010; 6 (2): 403-408.
[16]. Montalbetti C AGN, Falque V. Amide bond formation and peptide coupling. Tetrahedron 2005: 61 (46): 10827-10852.
[17]. Vijayabaskar V, Tikku VK, Bhowmick AK. Electron beam modification and crosslinking: Influence of nitrile and carboxyl contents and level of unsaturation on structure and properties of nitrile rubber. Radiat Phys Chem 2006; 75 (7): 779-792.
[18]. Sudhamani SR, Prasad MS, Udaya Sankar K. DSC and FTIR studies on Gellan and Polyvinyl alcohol (PVA) blend films. Food Hydrocolloid 2003; 17 (3): 245-250.
[19]. Majumder PS, Bhowmick AK. Surface-and bulk-properties of EPDM rubber modified by electron beam irradiation. Radiat Phys Chem 1999; 53 (1): 63-78.
[20]. Hashimoto D, Hirota M, Yagi Y, Baba H. Hyaluronate carboxymethylcellulose-based bioresorbable membrane (Seprafilm) reduces adhesion under the incision to make unplanned re-laparotomy safer. Surg Today 2012; 42 (9): 863-867.
[21]. Yu SL, Singh S, Chen HW, Chen HY, Chen JJW, Chen WJ, Chen HS, Chen SC. Intra-abdominal adhesion formation induces anti-oxidative injury, enhances cell proliferation, and prevents complement-mediated lysis. Wound Repair Regen 2008; 16 (3): 388-398.
[22]. Pismensky SV, Kalzhanov ZR, Eliseeva MY, Kosmas IP, Mynbaev OA. Severe inflammatory reaction induced by peritoneal trauma is the key driving mechanism of postoperative adhesion formation. BMC Surg 2011; 11 (1):30

[23]. Corona R, Verguts J, Schonman R, Binda MM, Mailova K, Koninckx PR. Postoperative inflammation in the abdominal cavity increases adhesion formation in a laparoscopic mouse model. Fertil Steril 2011; 95 (4): 1224-1228.
[24]. Hering TM, Marchant RE, Anderson JM. Type V collagen during granulation tissue development. Exp Mol Pathol 1983; 39 (2): 219-229.
[25]. Molinas CR, Binda MM, Koninckx PR. Angiogenic factors in peritoneal adhesion formation. Gynecol Surg 2006; 3 (3): 157-167.
[26]. Moraloglu O, Işik H, Kiliç S, Sahin U, Caydere M, Ustün H, Batioglu S. Effect of bevacizumab on postoperative adhesion formation in a rat uterine horn adhesion model and the correlation with vascular endothelial growth factor and Ki-67 immunopositivity. Fertil Steril 2011; 95 (8): 2638-2641.

研究主題二：In vitro properties of gellan gum sponge as the dental filling to maintain alveolar space

Abstract

The insertion of dental filling into the dental cavity is a common method of maintaining the space and shape of dental cavities after dental extractions. To develop novel dental fillings meeting clinical requirements, gellan gum (GG) is selected in this study to prepare fillings with specific characteristics by modulating gellan gum concentrations (denoted as GG-DF). The results indicate that the microstructure, porosity, and compression modulus of 1.5% and 1.75% GG-DF are similar to a commercially product (TeruplugR) and with good blood absorption capacity. The degradation ratio of TeruplugR in an amylase/ phosphate buffer solution after 4 weeks is 80% whereas that of 1.5% and 1.75% GG-DF is 65%. Cell migration studies confirmed that the migration ability of fibroblast was significantly inhibited by gellan gum. These results demonstrate that 1.5% and 1.75% GG-DF are potentially viable for developing into dental fillings.

1. Introduction

There are risks involved in the decay and resorption of alveolar bony tissue upon exodontias, tooth extraction, traumatic injuries or endodontics because of a lack of on-site physiological treatment. In general, the alveolar bone may atrophy 40 % to 60 % in two years after a tooth is removed without appropriate therapy (Cawood, & Howell, 1998; Devlin, & Sloan, 2002). Furthermore, damage or degeneration of the jaw bones may cause loosening or even the loss of other teeth. When a patient is

considering having a tooth implantation, a proper protective procedure to reserve space for ossification may be required (Bodic et al., 2005; Szabo et al., 1997). Without treatment, problems occur because the gingival tissues heal faster than the alveolar bony tissues. To protect the original vacancy and to prevent excessive growth of gingival tissues from occupying the space for the alveolar bone after tooth extraction, some products that function as dental fillings or dental plugs have been utilized to provide protection and retain the space for alveolar bone cells to gradually grow into (Accorinte et al., 2008; Serino, & Biancu, 2003; Wand, & Tsao, 2007).

The ideal materials used to prepare a dental filling should have three characteristics. First, the filling is required to have proper compressibility in order to allow proper control during the void-filling procedure. An ideal resorptive dental protective filling should behave like a sponge with good compressibility and easy fill into the dental cavity. Second, proper resorption time is required, which is typically one year for osteoblasts to mature and of the total ossification of a wound. In clinical practice, a minimum of at least 4 weeks of retaining proper protective capability is required for a dental filling. If the resorption time of the filling is too short, the gingival tissues will occupy the space reserved for the alveolar bony tissues to grow into. Finally, the filling must be capable of protecting the wound and promoting hemostasis. Clinically, exodontias procedures usually induce massive bleeding and salivating. A dental filling should adsorb blood and stop bleeding readily while consolidating alveolar bone after a tooth extraction. Currently commercial dental filling (Teruplug ®) are mainly made of collagen. Collagen, although an excellent biocompatible material that promotes tissue regeneration, is disadvantageous because it is mechanically weak, quickly degrades and extremely expensive. In this study, we aimed to find an alternative material that meets the requirements of being clinically friendly, readily adsorptive and yet inexpensive for dental applications.

Gellan gum (GG), which is also known as polysaccharide S-60, is produced by a non-pathogenic strain of *Pseudomonas elodea*. Its main chain consists of four repeating carbohydrates, including two D-glucose, one L-rhamnose, and one D-glucuronic acid. Currently, GG (a biodegradable and food additive approved by the FDA) is extensively used in the food industry (Karim, & Bhat, 2008), but it has rarely been investigated for biomedical applications except for use in drug delivery (Babu et al., 2010). Because GG is an anionic polysaccharide, it could act to prevent cell adhesion. Our previous studies have shown that GG film could effectively act as a barrier, inhibiting the growth of fibroblasts at wound sites (Lee et al., 2010). In this study, we prepared water-insoluble GG sponges and evaluated the potential applications in dentistry. We explored its basic properties, including molecular structure, water content, porosity, compression modulus, blood absorption,

degradation behavior and wound closure, and compared them to commercial product.

2. Methods

2.1 Fabrication of the Gellan gum dental filling

Various weights of Gellan gum (GG) were dissolved in 100 ml of deionized water and heated at 85-90℃ until they became transparent solutions. The concentration (wt/vol) of GG solutions were 0.75%, 1%, 1.25%, 1.5% and 1.75%. Then, 2 mL of GG solution were poured onto petri dishes (diameter 1.1 cm), frozen at -20°C overnight and lyophilized to obtain a 3D sponge (denoted as 0.75% GG-DF, 1% GG-DF, 1.25% GG-DF, 1.5% GG-DF, 1.75% GG-DF). The resultant porous GG-DF sponges were then cross-linked by immersing them into the deionic water containing 15 mM 1-ethyl-3-(3-dimethylaminopropyl) carbodiimide for 24 h at room temperature. The treated GG-DF sponges were washed with distilled water three times, frozen at -20°C and lyophilized again.

2.2 Morphology characterization

Scanning electron microscopy (SEM) (FEI Quanta 400 F) was employed to examine the morphology of the GG-DF and commercial product (Teruplug ®) with an emphasis on the porous characteristics. Prior to SEM, the samples were sputter-coated with gold.

2.3 Water content

The water content of the GG-DF and the Teruplug ® was determined by swelling the plugs in phosphate buffered saline (PBS) at pH 7.4 for 2 h at room temperature. The wet weight (W_{wet}) of the swollen sponge was measured immediately after gently blotting with filter paper to the remove surface liquid and then lyophilizing and reweighing (W_{dry}) the sponge. The water content of the plug was calculated using the formula (Lee, Hung, Cheng, Wang, 2005):

$$WC = (W_{wet} - W_{dry}) / W_{wet} \times 100\%$$

2.4 Determination of Porosity

The porosity of the GG-DF and Teruplug ® was determined using Archimedes' principle (Wan et al., 2008). The exterior volume (V_s) of the plug (1 cm × 1 cm) was measured using a Vernier caliper. The sample was then immersed in a pycnometer containing 99% ethanol solution. The actual volume (V_a) of the sample was calculated using the formula:

$$V_a = [(W_w - W_o) - (W_t - W_p)] / (0.789\ g/cm^3)$$

where W_w is the weight of the ethanol and the pycnometer, W_o is the dry weight of the pycnometer, W_t is the combined weight of the ethanol, the pycnometer and the

plug sample, W_p is the combined weight of the dry pycnometer and dry plug sample, and 0.789 g/cm^3 is the density of 99% ethanol solution. The porosity of the plug was then determined using the following formula:

$$\text{Porosity } (\%) = (V_s - V_a) / V_s \times 100\%$$

Porosity values were expressed as means ± standard deviations (n = 3).

2.5 Mechanical properties measurement

To assess the effect of various gellan gum concentrations on the mechanical properties of the dental fillings, compression tests were performed on an Instron (MODEL: JTM-S230) mechanical tester. The GG-DF and Teruplug ® sponges (1 cm thick, 8 mm in diameter, n=5) were compressed in the direction normal to the circular face of the cylindrical samples at a rate of 2 mm per minute until the sponge failed. The Young's modulus was defined as the slope of the linear region of the stress-strain curve in the 5-15% of the strain range. Ultimate stress and ultimate strain values were taken as the point where the sponge failed.

2.6 In Vitro Degradation Test

The in vitro degradation tests of the GG-DF and Teruplug ® were conducted by incubating the fillings in 5 ml of amylase (20 U) and 5 ml of PBS solution on a shaker set at 40 rpm and 37℃. At predetermined time intervals, the filling was taken out of the incubation medium, washed with distilled water and dried, and the weight of the filling was measured. Another 5 ml of amylase solution and 5 ml of PBS solution were added into the vial, and the test resumed. The degradation profiles were expressed as the accumulated weight losses of the fillings:

$$\text{Degradation percentage } (\%) = 100-(Wo-Wt)/Wo\times100\%$$

where Wo is the sample original weight and Wt is the sample dry weight after degradation.

2.7 Absorption and blood clotting testing

The absorption rate of the GG-DF sponges was determined using human whole blood. The latter was obtained from the Taiwan Blood Services Foundation (TBSF, Taipei, Taiwan). GG-DF sponges were cut into 1 cm × 1 cm squares and placed into glass bottles. Then, 0.4 mL of human whole blood was dispensed onto the dressing. The absorption rate was defined as the time required for the dispensed fluid to be completely absorbed by the sponge (Kang et al., 2011).

The blood clotting test was modified from Ong, Wu, Moochhala, Tan, & Lu (2008). Sponges were cut into 1 cm × 1 cm squares and placed into glass bottles.

Next, 0.25 mL of human whole blood (containing the anticoagulant citrate dextrose at a 1:6 ratio) was slowly dispensed onto the surface of the dressings. The bottles containing the samples were then incubated at 37 °C. After a predetermined amount of time (30 and 60s), 20 mL of distilled water was carefully added by dripping water down the inside wall of the bottles, to prevent disrupting the clotted blood. Red blood cells that were not entrapped in the clot were hemolyzed with distilled water, and the absorbance of the resultant hemoglobin solution was measured at 540 nm (UV-VIS spectrophotometer Agilent 8453, Santa Clara, CA, USA). The absorbance of 0.25 mL of whole blood in 20 mL of distilled water was used as a reference value. We also observed the morphology of blood coagulation by SEM. A sample of 0.5 mL of human whole blood was added to the GG-DF or Teruplug ®. After incubating at 37 °C for a predetermined amount of time, the sponges were fixed, dried and sputter-coated with gold for SEM studies.

2.8 Wound closure assay

The wound closure assay was a modification of the Platypus Technologies Oris Cell Migration Assay (Abingdon, UK) (Carragher, & Frame, 2011). Each well of an Oris 96-well plate was prepared as follows: The center of the well was coated with 1 mg/ml of gellan gum or 1 mg/ml of collagen and allowed to dry for 24 h. Then, a stopper was placed in the well to cover the material coated zone. L929 fibroblasts (cell density 5×10^4/ml) were seeded onto the plating medium in this outer area. On day 2, the plugs were removed. After 12 and 48 h, cells were stained with Giemsa stain (Sigma-Aldrich, Dublin, Ireland). The Oris 'detection mask' was used to visualize the wound area, which was photographed.

3. Results and discussion

3.1 Morphologies and porosity of the GG-DF sponges

Morphology and SEM images of GG-DF sponges are shown in Fig.1 and Fig.2. The sponge samples have a pore size between 200 and 300 μm^{-1} and vary with the GG solution concentration. The porous diameter decreases with a decreasing concentration of GG solution. This relationship occurs because higher GG solution concentrations have higher viscosity (Hsieh et al., 2007); therefore, it is easy to maintain smaller pore diameter after lyophilizing. Porosity was calculated from the equation in section 2.4. As shown in the table 1, porosity decreases with an increasing GG solution concentration. The 95%-24% porosity could be obtained by controlling the concentration of GG. From these results it is evident that 1.5% GG-DF, 1.75% GG-DF and Teruplug ® have similar morphologies and porosity profiles.

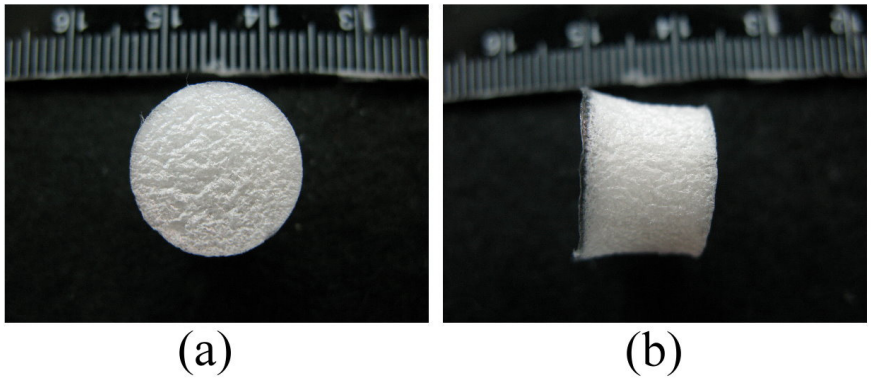

Fig.1. Morphology of the 1.5% GG-DF (a) front view, (b) side view.

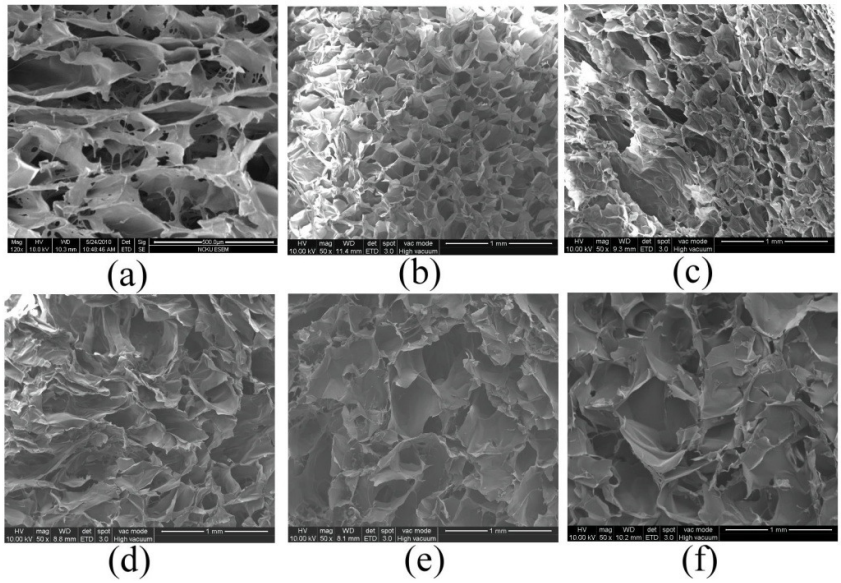

Fig.2. SEM micrographs of the cross-section of the dental fillings: (a) Teruplug ® , (b) 0.75% GG-DF, (c) 1.0% GG-DF, (d) 1.25% GG-DF, (e) 1.5% GG-DF, (f) 1.75% GG-DF.

3.2 Water absorption

To maintain the GG-DF shape for the socket filler, the degree of water absorption is important. High water absorption sponge may absorb excess water and expand, causing deformation. Table 1 shows water absorption ration of sponges produced under various concentrations of GG. With an increase in the GG solution concentration, the capacity of water absorption is reduced. The capacity of water absorption of GG sponge is closely related to the porosity. Some studies have indicated that scaffolds with higher porosity have increased water storage space and would thus have a higher capacity of water absorption (Davidenko et al, 2010). Other studies have suggested that smaller pore sizes cause increased capillary phenomenon

leading to increased water absorption. In this study, we could see similar results from other papers. The most appropriate water absorption ratio for a sponge as a socket filler is not yet known. Compared with the commercial product, we noted that the 1.75% GG-DF and Teruplug ® had similar water absorption capacity and about 92%.

Table 1 : Porosity and Water absorption capacity of DD-GF

Designation	Porosity (%)	Water absorption (%)
0.75% DD-GF	95.54±11.26%	96.9 ±0.19%
1% DD-GF	85.4±21.17%	96.9 ±0.19 %
1.25% DD-GF	66.27±8.03%	97 ±0.54%
1.5% DD-GF	28.98±4.53%	96.2 ±0.64%
1.75% DD-GF	20.61±2.9%	92 ± 0.10%
Teruplug ®	38.9±1.5%	92.2 ± 4.7%

3.3 Mechanical properties

An ideal resorptive dental protective material should have good compressibility in order for the clinician to easy fill into the dental cavity. The slopes of the compressive stress–strain curves from 0% to 5% deformation were used to calculate the compressive modulus. As shown in Table 2. The results indicate that with increasing GG solution concentration, the Young's modulus and maximal shear stress (τ_{max}) both increase. The compressive moduli of the sponges of 0.75%, 1%, 1.25%, 1.5% and1.75% GG-DF are 3.4, 4.2, 8.6, 15.9 and 21.1 MPa, respectively. It is known that compressive strength and Young's modulus increase with decreasing porosity (Jang, & Matsubara, 2005). In addition, previous studies have indicated that the Young's modulus of the porous sample significantly increases as the amount of material in the network increases. Therefore, the GG sponge's mechanical properties are primarily determined by the concentration of GG. From the results, we also find that the mechanical properties of 1.5% and 1.75% GG-DF are similar to Teruplug ®.

Table 2: Mechanical properties of GG-DF

Designation	τ_{max} (MPa)	Compressive modulus (MPa)
0.75% GG-DF	0.31±0.02	3.4
1% DD-GF	0.594±0.07	4.2
1.25% DD-GF	1.04±0.07	8.6

1.5% DD-GF	1.75±0.15	15.9
1.75% DD-GF	2.11±0.1	21.1
Teruplug ®	1.48±0.24	18.5

3.4 In vitro degradation

An intrinsic characteristic of natural polysaccharides is their ability to degrade through the actions of naturally occurring enzymes that are present in the serum and saliva. Therefore, it is of particular interest to study the enzymatic degradation of GG-DF sponges prepared by different GG solution concentrations. GG is a linear polysaccharide that is composed of glucose-rhamnose-glucuronic acid units bonded by α(1-4) glycosidic links. Fig.3 shows the degradation rate of the GG-DF sponges and Teruplug ® at a pH of 7.4 in the presence of α-amylase. The control sample (Teruplug ®) and 0.75% GG-DP each with a significant weight loss during the first week, but other samples degraded at a slower rate. The degradation ratio of Teruplug ® in the amylase solution after 4 weeks was 80 %, and that of 1.5 % and 1.75% GG-DF was 65 %. To maintain the alveolar space**,** a minimum of about 4 weeks duration is required. The results indicate that with increasing GG concentration, the degradation rate decreased. Therefore, the degradation rate of the GG-DF sponge can be controlled for clinical requirements by varying the concentration of GG.

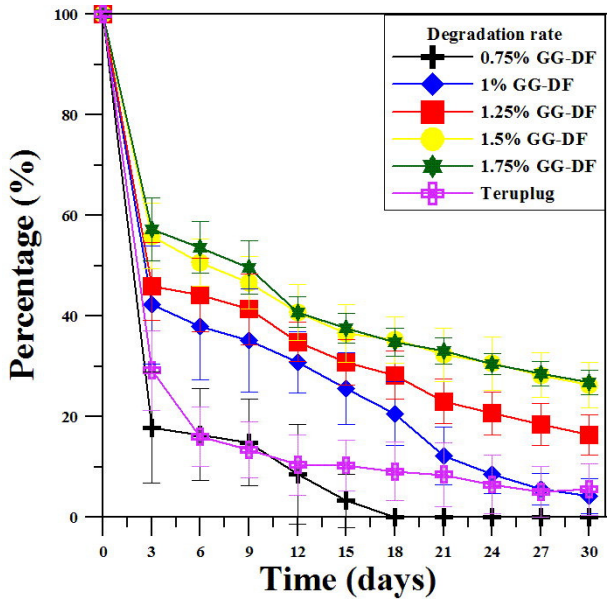

Fig.3. Degradation of Teruplug ® and GG-DF in amylase solution.

3.5 Blood absorption

The GG-DF demonstrated higher blood absorption rates compared with Teruplug ®.

When 1.5% GG-DF sponges were placed into 0.25 mL of human whole blood for 60 seconds, the absorbance of the remaining hemoglobin not absorbed into the sponge was reduced from 1.8 (at t=0) to 0.8 OD. This result indicates that about 66% of RBC was absorbed by the 1.5% GG-DF sponge. In contrast, about 55% RBC were absorbed by the Teruplug ®. The blood absorption capacity of the 1.5% GG-DF sponge may be attributed to its extensive porous structure. To assess blood coagulation, the sponges with absorbed blood were placed in 0.9% saline solution. As shown in Fig.4, the Teruplug ® swelled significantly in saline, and blood leakage from the sponge was observed. This result was not observed with the 1.5% GG-DF sponge, which indicates that the blood was well confined inside the 1.5% GG-DF. The SEM evaluation of blood clot formation on the 1.5% GG-DF sponge and Teruplug ® revealed that red blood cells formed aggregates (Fig.5a & 5b). More specifically, the red blood cells coalesced into an erythrocyte clot in both the 1.5% GG-DF sponge and Teruplug ® (Kang et al., 2011).

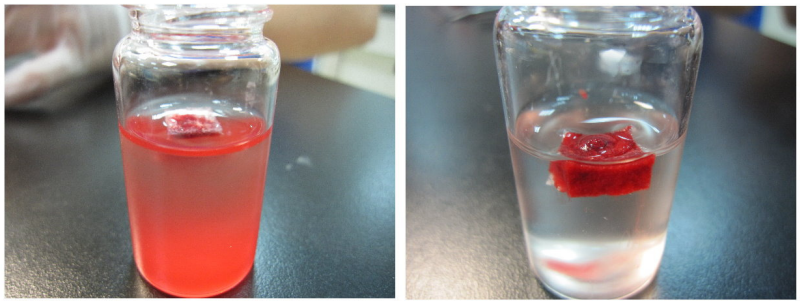

Fig.4. Photographs showing that more haemoglobin leaked from the Teruplug ® (left) than from the 1.5% GG-DF (right).

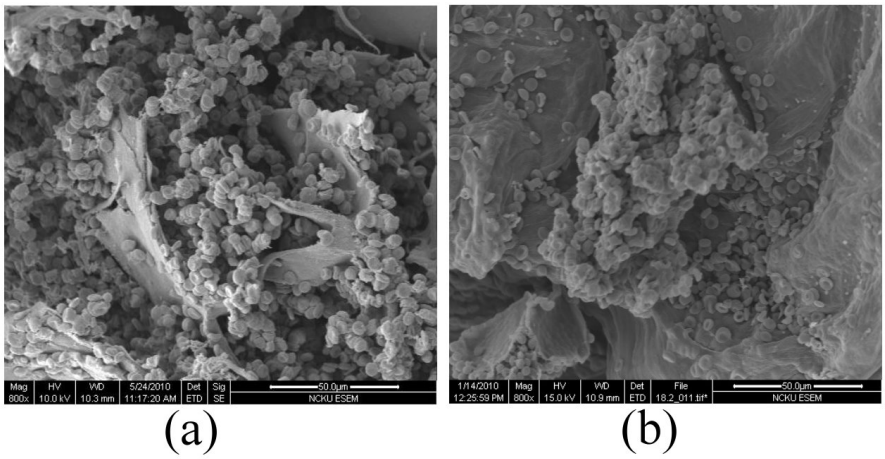

Fig.5. SEM micrographs of human whole blood on the (a) Teruplug ®, (b) 1.5% GG-DF after 60s of absorption.

3.7 Wound healing

An ideal resorptive dental protective material should prevent gingival fibroblast growth and migration into the alveolar space (Chang et al., 2010**;** Chung et al., 2009**).** The effect of inhibiting fibroblast migration with GG was investigated by a wound healing assay. The wound healing migration assay is an established and widely used procedure that allows monitoring cell migration at different intervals of time in response to an artificial wound produced on the cell monolayer. In addition, this method allows the observation of changes in cell morphology occurring during this process. As the photos show, fibroblasts migrated to the central barren spot after 12 h incubation and nearly filled it after 48 h incubation (Fig.6). When the center of the well was coated with 1 mg/ml collagen, fibroblasts also migrated to the central barren spot after 12 h of incubation. However, if the center of the well was coated with 1 mg/ml GG, fibroblast migration was significantly inhibited. The mechanism by which the GG caused the significant reduction in cell migration is not clear; however, the reduction is likely due to the negative charge of GG.

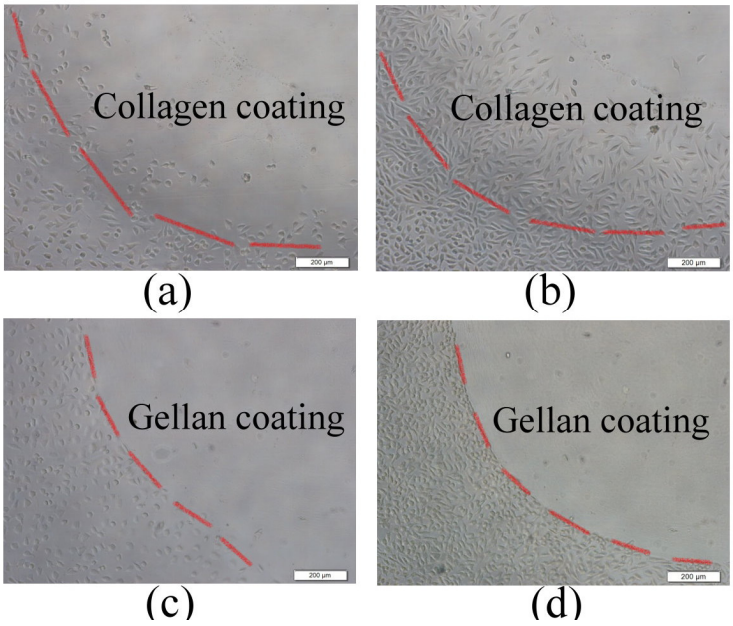

Fig.6. Cell migration as measured by microscopy. The analytic zone into which cells have migrated is separated by the red dotted line. (a,b) fibroblasts migrated after 12 and 48h (collagen coating), (c,d) fibroblasts migrated after 12 and 48h (gellan gum coating).

4. Conclusion

The maintenance of dental cavities after a dental extraction (also termed alveolar ridge preservation) is crucial for the success of dental implants and prosthetics. GBR is the most common alveolar ridge preservation technique because it is easy to

perform and generates favorable results. One of the GBR procedures is to insert bone graft materials into dental cavities to preserve the space (Marukawa et al., 2011). The function of bone graft materials is to prevent atrophy of the alveolar ridge and alveolitis, as well as to stop bleeding. The best choice of bone graft material is autologous bone; however, autologous bone is limited in supply and is difficult to obtain. Allogeneic bone is an alternative source of bone graft material and is easy to obtain, but it produces unstable effects. Therefore, the development of synthetic material with good biocompatibility is advantageous. Teruplug ® is a commercial product that is presently used for preserving dental cavities. It consists of a 3D spongy structure manufactured with dense collagen fibers. Because of its plasticity, Teruplug ® can be inserted into a wound created by a dental extraction to preserve the space generated by the procedure. Additionally, Teruplug ® has a hemostatic function, and can prevent massive bleeding after a dental extraction while generally having good biocompatibility. However, controlling the degradation characteristics of Teruplug ® can be challenging, and its high cost limits its clinical applications.

In this study, we used microbial GG as the substrate and prepared fillings for dental cavities with various characteristics by modulating GG concentrations. Through structural property analysis, we demonstrate that the microstructure, porosity, and compression modulus of 1.5 % and 1.75 % GG-DF are similar to those of Teruplug ®. Through *in vitro* degradation tests, we have verified that the degradation of GG dental cavity fillings can be regulated by the GG concentration. In the presence of amylase activity, 1.5 % and 1.75 % GG-DF can endure for an extended period of time (more than 4 weeks), while Teruplug ® can only endure for 2 weeks. Furthermore, 1.5 % GG-DF was subjected to blood absorption tests, and the results indicate that GG-DF dental fillings have better blood absorption capability than Teruplug ®. The high rate of blood absorption was attributed to hemocytes aggregating in the pores of the GG-DF sponge. Hemagglutination mechanisms were not examined in this study, and further investigations are required to determine whether GG sponges have hemostatic capacity. Another key to successful GBR is the prevention of epithelial cells and fibroblasts from migrating into dental cavities in order to preserve the shape of dental cavities. Through cell migration studies, GG was found to have superior inhibitory activities on cell migration. At present, no standards regarding dental filling quality are available for clinical evaluation. To evaluate the feasibility of the novel GG dental filling in this study, a commercially available product was chosen as a control. On the basis of the results observed, we conclude that of 1.5% GG-DF prepared in this study appeared to be of great potential for development into dental fillings.

Reference

1. Accorinte, M.L.R., Holland, R., Reis. A., Bortoluzzi, M.C., Murata, S.S., Dezan, E., Souza, V., and Alessandro, L.D. (2008). Evaluation of mineral trioxide aggregate and calcium hydroxide cement as pulp-capping agents in human teeth. *Journal of Endodont*, 34**,** 1-6.
2. Babu, R.J., Sathigari, S., Kumar, M.T., Pandit, J.K. (2010). Formulation of controlled release gellan gum macro beads of amoxicillin. *Current drug delivery*, 7 (1), 36-43.
3. Bodic, F., Hamel, L., Lerouxel, E., Baslé, M.F., and Chappard, D. (2005). Bone loss and teeth – Review. *Joint Bone Spine,* **72,** 215–221.
4. Carragher, N.O., Frame, M.C. (2011). Modelling distinct modes of tumour invasion and metastasis. *Drug Discovery Today: Disease Models*, 8(2-3), 103-112.
5. Cawood, J.I., and Howell, R.A. (1998). A classification of edentulous jaws. *International Journal of Oral and Maxillofacial Surgery,* 17, 232-236.
6. Chung, J.H., Nam, J.W., Kim, K.W. (2009). Effects of atelocollagen sponge (Teruplug ®) insertion on the periodontal healing of second molars after impacted mandibular third molar extraction. *International Journal of Oral and Maxillofacial Surgery*, 38 (5), 567.
7. Chang, S.J., Kuo, S.M., Liu, W.T., Niu, C.G., Lee, M.W., Wu, C.S. (2010). Gellan Gum Films for Effective Guided Bone Regeneration. Journal of Medical and Biological Engineering, 30, 99-103.
8. Davidenko, N., Campbell, J.J., Thian, E.S., Watson, J., Cameron, R.E. (2010). Collagen–hyaluronic acid scaffolds for adipose tissue engineering. *Acta Biomaterialia*, 6(10), 3957-3968.
9. Devlin, H., and Sloan, P. (2002). Early bone healing events in the human extraction socket. *International Journal of Oral and Maxillofacial Surgery*, 31, 641-645.
10. Hsieh, W.C., Chang, C.P., Lin, S.M. (2007). Morphology and characterization of 3D micro-porous structured chitosan scaffolds for tissue engineering. *Colloids and Surfaces B: Biointerfaces*, 57 (2), 250-255.
11. Jang, B.K., Matsubara, H. (2005). Influence of porosity on hardness and Young's modulus of nanoporous EB-PVD TBCs by nanoindentation. *Materials Letters*, 59 (27), 3462-3466.
12. Kang, P.L., Chang, S.J., Manousakas, I. Lee, C.W., Yao, C.H., Lin, F.H., Kuo, S.M. (2011). Development and assessment of hemostasis chitosan dressings. *Carbohydrate Polymers*, 85 (3), 565-570.
13. Karim, A.A., Bhat, R. (2008). Gelatin alternatives for the food industry: recent developments, challenges and prospects. *Trends in Food Science & Technology*,

19 (12), 644-656.

14. Lee, M.W., Chen, H.J., Tsao, S.W. (2010). Preparation, characterization and biological properties of Gellan gum films with 1-ethyl-3-(3-dimethylaminopropyl) carbodiimide cross-linker. *Carbohydrate Polymers*, 82 (3), 920-926.
15. Lee, M.W., Hung, C.L., Cheng, J.C., Wang, Y.J. (2005). A new anti-adhesion film synthesized from polygalacturonic acid with 1-ethyl-3-(3-dimethylaminopropyl) carbodiimide crosslinker. *Biomaterials*, 26 (18), 3793-3799.
16. Marukawa, K., Ueki, K., Okabe, K., Nakagawa, K., Yamamoto, E. (2011). Use of self-setting α-tricalcium phosphate for maxillary sinus augmentation in rabbit.*Clinical oral implants research*, 22 (6), 606-612.
17. Ong, S.Y., Wu, J., Moochhala, S.M., Tan, M.H., Lu, J. (2008). Development of a chitosan-based wound dressing with improved hemostatic and antimicrobial properties. *Biomaterials*, 29 (32), 4323-4332.
18. Serino, G., and Biancu, S. (2003). Ridge preservation following tooth extraction using a polylactide and polyglycolide sponge as space filler: a clinical and histological study in humans. *Clinical Oral Implants Research*, 14, 651-658.
19. Szabo, G., Suba, Z., and Barabas, J. (1997). Use of bioplant HTR synthetic bone to eliminate major jawbone defect: long-term human histolotical examinations. *Journal of Cranio-Maxillofacial Surgery*, 25, 63-68.
20. Wand, H.L., and Tsao, Y.P. (2007). Mineralized bone allograft-plug socket augmentation: rationale and technique. *Implant Dentistry*, 16, 33-41.
21. Wan, Y., Wu, H., Cao, X., Dalai, S. (2008). Compressive mechanical properties and biodegradability of porous poly (caprolactone)/chitosan scaffolds. *Polymer Degradation and Stability*, 93**,** 1736–1741.

主題三：Photocrosslinkable gellan gum film as an anti-adhesion barrier

Abstract

The purpose of this study was to develop a gellan gum-based film using a photocross-linker for medical applications. Gellan gum was grafted with cinnamate to yield a photocrosslinkable polymer. Gellan gum-cin had 14.7% of its D-galacturonic residues react with cinnamate groups and displayed maximum absorption at 254 nm. Investigation of the photochemical properties showed that the crosslinking efficiency was 82% after 16 min of UV irradiation. The anti-adhesion films prepared from gellan gum-cin polymers exhibited high gel contents (88 ± 2 %) and suitable mechanical properties. When implanted into rats, the gellan gum-cin film exhibited the most promising anti-adhesion potential in 2 out of 10 rats without forming any tissue adhesion. Furthermore, the gellan gum-cin film could effectively inhibit inflammation in rats based on the results of fluid leukocyte analyses. The gellan gum-cin film thus has potential in clinical applications.

1. Introduction

Gellan gum is a linear, anionic extracellular polysaccharide from Pseudomonas elodea with repeating tetrasaccharide units of D-glucose, D-glucuronic acid, D-glucose, and L-rhamnose (Jansson et al., 1983; O'Neil et al., 1983). Gellan gum is a food additive that functions as a stabilizer, thickening agent, and structuring and versatile gelling agent in a wide variety of foods. Recently, gellan gum has been investigated as a candidate material for biomedical engineering because of its biocompatibility and low cytotoxicity (Silva-Correia et al., 2011; Oliveira et al., 2010). Gellan gum has also been tested as a drug-delivery carrier, cell carrier, guided bone-regeneration material, and wound dressing (Lee et al., 2010; Chang et al., 2010). The stable cross-linked structure of gellan gum can be obtained in the presence of metallic cations or by forming bonds between gellan gum molecular chains and chemical cross-linkers, such as 1-ethyl-3-(3-dimethylaminopropyl) carbodiimide (EDC). Although the polysaccharide can be cross-linked with Ca^{2+} ions, the mechanical properties of polysaccharide are fragile and less malleable (Ichibouji et al., 2009). When implanted, tissue calcification occurs, which limits the biomedical application of Ca^{2+}–cross-linked gellan gum. In addition, chemical cross-linkers can be cytotoxic due to dosage responses and cross-linker residues (Powell & Boyce, 2006).

To develop a non-toxic method of cross-linking gellan gum that can be applied in biomedicine is the main purpose of this research work. Crosslinking via the photodimerization of polymeric systems has been utilized in various applications. In this study, we designed a new photocrosslinkable gellan gum molecule that contains a cinnamate moiety and may be used for medicinal purposes. The crosslink mechanism

is based on the π-electron density of the photoactive chromophore, with dimerization of the cinnamate groups occurring presumably as a result of [2+2]π-electron cycloaddition (Dong et al., 2005). The reaction does not require the addition of a light-sensitive initiator. Cinnamate is a natural tropane alkaloid found within the Erythroxylum coca plant that possesses anti-inflammatory and non-toxic properties (Ballabeni et al., 2010). In this study, cinnamate functions not only as a cross-linking agent but also as an anti-inflammatory drug.

Various types of films made of polysaccharides have been reported to reduce adhesion formation, including Dextran-70, Interceed and Seprafilm™ (Robertson et al., 2010), but have not fully satisfied the requirements for clinical implementation. An ideal adhesion-prevention product should be resolvable, non-reactive, easy to apply and capable of being fixed. In a previous study, we demonstrated that gellan gum could prevent fibroblast adhesion and migration. In this report, we describe the evaluation of the efficacy of a photosensitive gellan gum film (denoted as GG-Cin film) in reducing postoperative adhesion formation in a rat model.

2. Methods

2.1. Dissolution of gellan gum in Dimethyl Sulfoxide (DMSO)

To render gellan gum soluble in DMSO, the sodium ions of gellan gum were exchanged with the lipophilic tetrabutylammonium (TBA) ion (Oudshoorn et al., 2007). Ion exchange was performed using Dowex® 50W-X8 cation-exchange resin (1.8 mmol/g exchange capacity; Fluka 44519). The Dowex® resin was incubated with a large excess of TBA (1:2.77 molar ratio of the exchange capacity of Dowex® to TBA) dissolved in 50 ml deionized water for 1 h and washed extensively with water. Next, the resin was transferred into 1% (w/w) gellan gum solution in water (1:10 molar ratio of the carboxyl groups of gellan gum to Dowex®-TBA) and mixed for 2 h at room temperature. The mixture was then centrifuged for 10 min at 3000 rpm to remove the resin. The obtained gellan gum-TBA solution was lyophilized and used for chemical modification with a photosensitive group.

2.2. Synthesis of gellan gum-cinnamate in DMSO

Gellan gum-TBA was dissolved in DMSO (1% w/w). Cinnamyl bromide was dissolved in DMSO to a concentration of 4% (w/w). A mixture of Gellan gum-TBA solution and cinnamyl bromide solution was stirred at 50℃ for 48 hrs. The mole ratio of cinnamate to gellan gum carboxyl residues was 5:1. The gellan gum-cinnamate (GG-Cin) product was purified by ethanol precipitation. The purified gellan gum-cin was analyzed by ^{1}H-NMR (500 MHz, Bruker Advance DRX500).

2.3. Photochemical properties of gellan gum-cin

The photoreactivity of gellan gum-cin was studied by dissolving it in DMSO to a concentration of 0.1% (w/v) and exposing to UV light at 254 nm using a mercury lamp (Cole-Parmer 9815-series lamps 100 watts) for different intervals of time. After each irradiation period (2 min), UV spectra were recorded on a scanning spectrophotometer (Milton Roy Spectronic 3000 array). The crosslinking efficiency was determined by calculating the percent conversion of photoactive chromophores using the following equation (Dong et al., 2005)：

$$\% \text{ crosslinking} = (A_t - A_0) / (A_\alpha - A_0) \times 100$$

where A_0, A_t, and A_α are respectively the absorbance values at time 0, time *t*, and time a after which no further changes were observed in the absorbance.

2.4. Preparation of gellan gum-cin film

Gellan gum-cin (0.2 g) was dissolved in 1.5 ml DMSO and then mixed with 13.5 ml deionized water. The solution was poured onto a glass dish (diameter 5 cm) and evaporated at 50 ℃ until the weight of the film was constant. To prevent dissolution of the non-cross-linked gellan gum-cin film in the aqueous solution, the film was immersed in ethanol and irradiated with UV light (Cole-Parmer 9815-series Lamps 100 Watts) for 30 min. The cross-linked gellan gum-cin film was washed with 95% ethanol three times and then dried at room temperature.

2.5. Characterizations of the cross-linked gellan gum-cin film

An electrical thickness tester (mitutoyo, MDC-25 SB) was used to measure the thickness of the gellan gum-cin film. We used the FTIR-L396A (Perkin-Elmer) to analyze the properties of the chemical functional groups of the cross-linked gellan gum-cin film. The analysis of the gel content of the cross-linked gellan gum-cin film was performed as follows. After drying, we weighed the cross-linked film (W_1) and then swelled it in DDW at 37 ℃ for 24 h. After removing the wet film from the solution, the film was dried in a vacuum oven for 12 h at 60 ℃ and then weighed again (W_2). The gel content (%) was 100 (W_2/W_1).

The gellan gum-cin film was cut into 1 cm × 5 cm pieces (Mathew & Abraham, 2008). We then used the H1-KS testing machine (Tinius Olsen) with a crosshead speed of 5 mm/min to measure the mechanical properties of the gellan gum-cin films and to automatically record the mechanical parameters.

2.6. Animal implant study

Twenty Sprague-Dawley rats (200–250 g) were tested in a surgical research laboratory. Aseptic midline laparotomies were conducted while the animals were anesthetized with 4% trichloroacetaldehyde monohydrate (1 ml/100 g). The distal 3

cm of the cecum and opposing abdominal wall were scraped with a scalpel until the serosal surface was disrupted and hemorrhaged but not perforated. The denuded peritoneal wall was then covered with a gellan gum-cin film (diameter: 1.0 cm). The rats in the control group were not covered with any anti-adhesion film. Contact between the cecum and opposing peritoneal wall was maintained in all animal groups with two nonoccluding loops of 4/0 polypropylene sutures placed 2 cm apart. After completion of the procedure, the abdomen was closed in a double layer using 4/0 polypropylene in a continuous fashion. The experimental rats were sacrificed on day 3 or 7 after surgery to examine the process of adhesion formation at the injured site (Peng et al., 2011). Adhesions were scored in a blinded manner according to the method of Zuhlke et al. (Table 1), where grade 0 indicates no adhesions and grade 4 indicates firm extensive adhesions that are dissectable only with sharp instruments and almost unavoidable organ damage. The abdominal wall of the injured site was removed and fixed in 10% formalin solution. The tissues were processed by the standard procedure for histological examinations, and their thin sections were examined after staining with hematoxylin–eosin (H–E).

Table 1：Grading of adhesion according to Zuhlke (grade description).

0	No adhesions
1	Filmy, fibrin adhesions, easily removed by blunt dissection (mild)
2	Fibrous adhesions, easily dissected (moderate)
3	Thick fibrous adhesions, dissectable (severe)
4	Thick fibrous adhesions, not dissectable without damage to the adherent tissue (very severe)

2.7. Peritoneal fluid analysis

Peritoneal fluids were collected before the operated animals were sacrificed on day 3 or 7 after surgery. The peritoneal fluid was aspirated through a pipette with a bulb tip after 3 ml of the DMEM containing heparin was injected into the peritoneal cavity. Turk's solution (0.01% Giemsa stain and 3% acetic acid) was used to stain white blood cells, and the number of neutrophils in the collected fluid was determined by cell counting using a hemocytometer.

2.8. Statistical analysis

Each of the experiments was repeated at least five times, and the values were

expressed as the means± standard deviations. For comparison between two groups of data, Student's t-test was performed. Differences were considered to be statistically significant at $p< 0.05$.

3. Results and discussion

3.1. NMR characterization of gellan gum-cin

We have developed a method to crosslink gellan gum using pendant photofunctional groups, such as cinnamate. Gellan gum was grafted with cinnamate to yield gellan gum-cin in DMSO. Gellan gum-cin polymers having α,β-unsaturated carbonyl groups in the backbone underwent crosslinking upon irradiation with UV light. The reaction mechanism is depicted in Fig. 1. The gellan gum-cin polymer was analyzed based on the ^{1}H-NMR spectra results (Fig. 2.). These results showed the presence of characteristic peaks that correspond to –CH of rhamnose (δ 5.2-5.6 ppm), -CH of glucuronic acid (δ 4.9-5.1 ppm), -CH of glucose (δ 4.0-4.8 ppm) and $–CH_3$ of rhamnose (δ 1.2 ppm) (Daniela F Coutinho et al., 2010). The spectrum confirms the incorporation of the cinnamate group by the presence of methylidyne proton peaks at 6.3 and 7.5 ppm and a phenyl proton peak at 7.2–7.5 ppm. The degree of cinnamate substitution can be conveniently determined by comparing the integrated intensity of the phenyl and –CH=CH– peaks of the cinnamate group to the integral of the $–CH_3$ protons（δ 1.2 ppm）of gellan gum. Accordingly, the degree of cinnamate substitution was approximately 14.7％ (Dong et al., 2005).

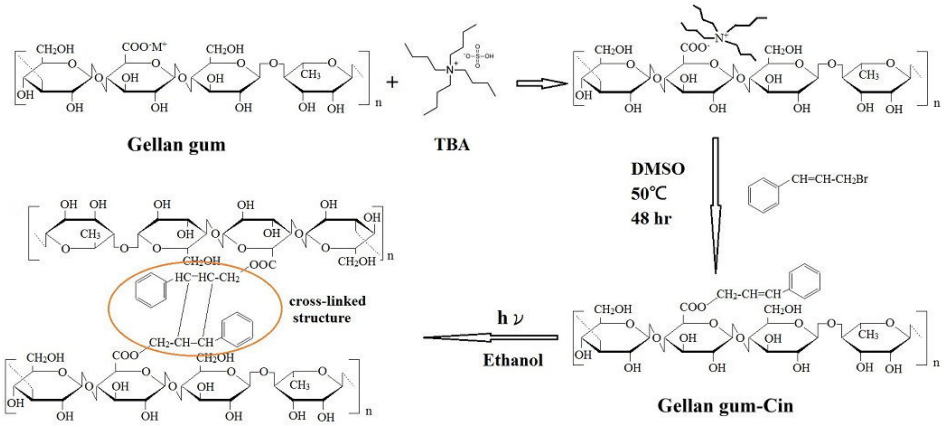

Fig.1. The photocrosslinking mechanism of gellan gum.

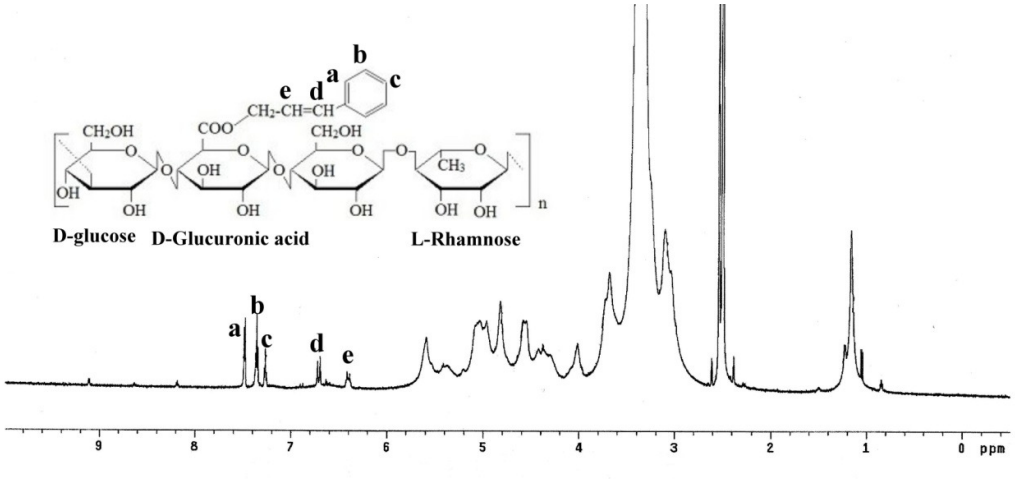

Fig. 2. NMR spectrum of gellan gum-cin.

3.2 FTIR characterization of gellan gum-cin

Fig. 3A and 3B shows the FTIR spectrograms of gellan gum and gellan gum-cin polymers. Fig. 3A shows the assignment of the absorption band at 3309 cm^{-1} to the stretching of the –OH groups in gellan gum (Sudhamani et al., 2003). The band at 2917 cm^{-1} is due to the stretching vibrations of the $–CH_2$ group, whereas the bands appearing at 1148 and 1015 cm^{-1} are due to ethereal and hydroxylic C-O stretching. The peaks at 1603 and 1403 cm^{-1} can be assigned to the characteristic absorption band of carboxyl in gellan gum. The bending vibration of C-H appears at 835 cm^{-1}. Fig. 3B shows the FTIR spectrogram of gellan gum-cin; the most prominent difference in the spectrum between gellan gum and gellan gum-cin appeared as a new absorption peak at 1734 cm^{-1}, which was assigned to the C=O ester group. The C=C stretching vibration of the benzene ring in the cinnamate groups appears at 1449 and 1491 cm^{-1} (Sung et al., 2004; Francisco et al, 2007). It also caused the absorption peak of the –OH groups to shift to a higher wave number, 3342 cm^{-1}, and that of the C-O stretching to shift from 1015 to 1011 cm^{-1}. These data indicate that the new absorption peak is not caused by residual cinnamate and confirms that the covalent grafting reaction was successful.

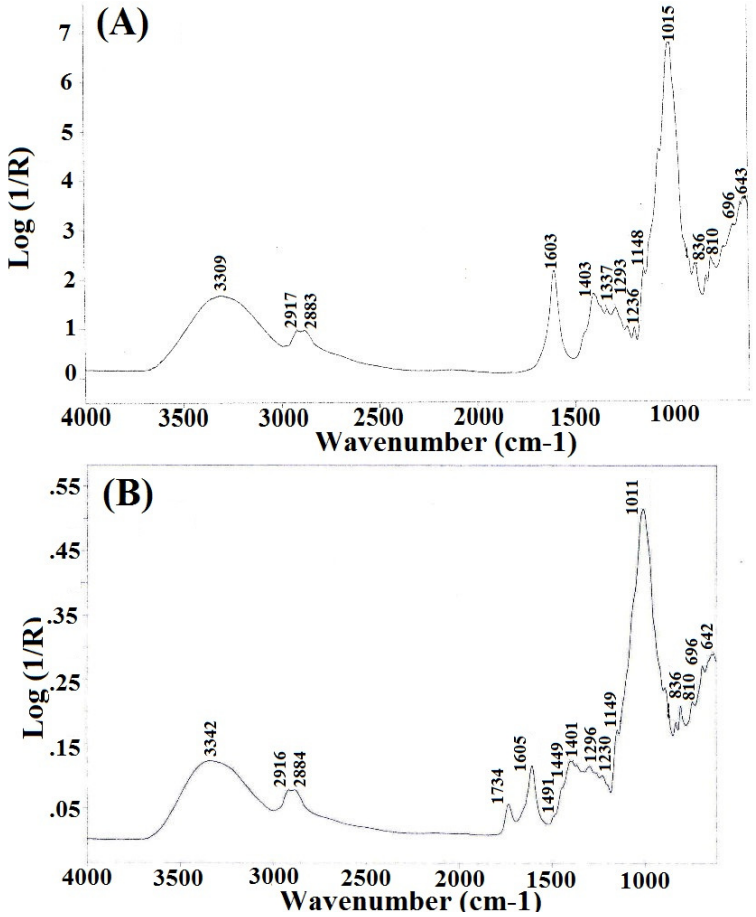

Fig.3. FTIR spectra of gellan gum (A) and gellan gum-cin (B).

3.3 Photoreactivity measurements

The UV spectrum of gellan gum-cin polymer is shown in Fig 4. Gellan gum-cin exhibited an absorption around 254 nm due to the π-π^* transition of the double band present in the polymer chain. When the gellan gum-cin polymer were subjected to the UV irradiation, there is a change in the UV absorption maximum at 254 nm due to the formation of cyclobutane ring. This cyclobutane ring formation is responsible for the decrease in the absorption upon irradiation with UV light. This type of decrease maximum upon irradiation was reported earlier (Watanabe et al., 1986). The photosensitive gellan gum polymers with pendant chalcone groups（α,β-unsaturated carbonyl）that undergo a【2+2】photocycloaddition reaction upon UV irradiation are regarded as negative-type photoresists (Nagata & Inaki, 2009; Allen Norman et al., 1993). The crosslinking efficiency of the gellan gum-cin increased with the duration of light irradiation, as shown in Fig. 5. Within 4 min, the crosslinking efficiency was 82% and was nearly complete within 16 min. These results suggest that a short exposure time was enough to induce the cross-linking reaction of the photopolymer.

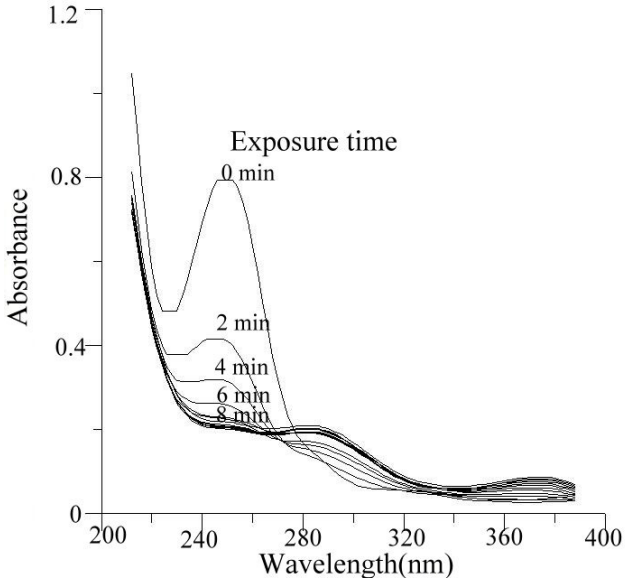

Fig.4. The change of UV spectra of the photosensitive gellan gum-cin induced by irradiation of UV light through filter.

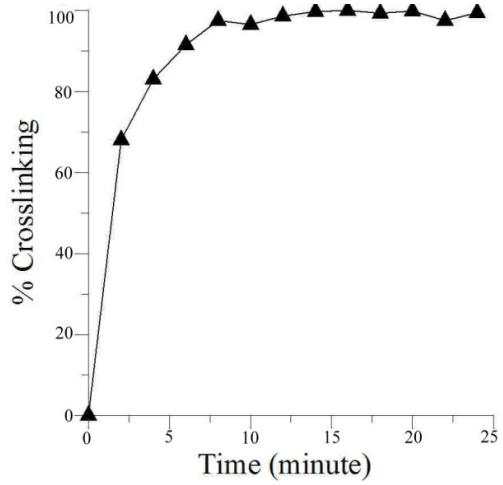

Fig.5. The effect of irradiation time of the extent of crosslinking of the gellam gum-cin.

3.4 Physical properties of crosslinked gellan gum-cin film

The gellan gum-cin film was crosslinked via short wavelength UV irradiation（254 nm）. The average thickness of the films was 24 ± 2 μm. The prepared film was soft, flexible, transparent and capable of being fixed in position. The gel content of a film is related to the crosslinking density of the film (Nagasawa et al., 2004). The crosslinked gellan gum-cin film had a high gel content of approximately 88 ± 2 %. However, the non-cross-linked gellan gum-cin film was rapidly swollen with water. For clinical use, the most important mechanical properties of anti-adhesion film are tensile strength and elongation. Mechanical testing revealed that the maximum tensile

strength and elongation at break of the non-UV-irradiated film were 31.4 ± 4.8 Mpa and 8.2%, respectively. The maximum tensile strength and elongation at break of the UV crosslinked film were 42.6 ± 6.1 Mpa and 6.8%. It was observed that tensile strength of the crosslinked film was slightly increased and the film became stiffer. Vijayabaskar et al. (2006) indicated that the tensile strength of a polymer is closely correlated to the density of cross-linking. At high cross-link density, the segments of macromolecules become immobile, which causes the system to become stiff and show a decrease in elasticity. At present, no standards regarding the mechanical properties of anti-adhesion films are available for clinical evaluation. In this study, the vivo evaluation of gellan gum-cin films for the prevention of postoperative adhesion showed that the films had sufficient mechanical strength and easy to apply.

3.5 In vivo evaluation of gellan gum-cin film for the prevention of postoperative adhesion

The occurrence of tissue adhesion between the cecum and the peritoneum was examined on the 3rd and 7th days after surgery. In the control group (without membrane), adhesion of the cecum to the peritoneal wall was found in 5 of the total 5 rats operated (adhesion incidences 100%) on day 3 and day 7 after surgery (Fig. 6a and 6b). The adhesion scores of the control group were between 3 (severe) and 4 (very severe). In contrast, the gellan gun-cin film effectively prevented tissue adhesion in all rats operated (5 rats operated) on day 3 after surgery and reduced adhesion incidences by 60% (3 out of 5 rats operated) on day 7 after surgery (Fig. 6c and 6d). The adhesion scores of the experimental group were between 0 (no adhesion) and 1 (mild). Superior anti-adhesion capabilities were demonstrated by the gellan gum-cin film throughout the observation period.

Tissues surrounding the injured sites were dissected and examined. Photomicrographs of the sectioned, H&E-stained tissues on the 3rd and 7th day of the repairing process are shown in Fig. 7. In the control group, newly formed dense adhesive tissue was found between the peritoneal wall and the mucosa of the cecum. The adhesion area was also covered by thick fibrous tissue and contained a thick layer of fibroblast. With the treated gellan gum-cin film, on the 3rd day after surgery, the surgical lesions had not completely healed and did not form adhesive tissue between the peritoneal wall and the mucosa of the cecum. On the 7th day after surgery, the tissues around the surgical lesions had almost completely healed. Histological observation showed that on the 3rd and 7th days following surgery inflammatory cells were found around the surgical lesions in all groups. The number of inflammatory cells was counted using a cell-counting method.

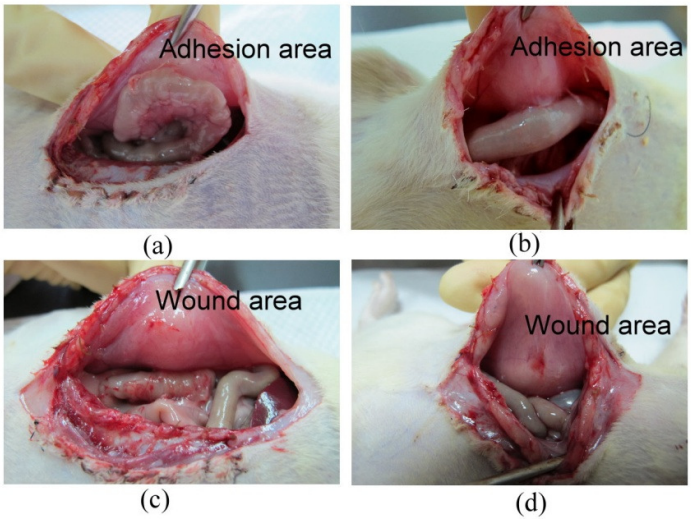

Fig.6. Repair of the injured sites between the cecum and the peritoneal wall in the operated rats 3 and 7 days after surgery：(a,b) adhesion formation (control group) and (c,d) treated with gellan gum-cin film without adhesion formation.

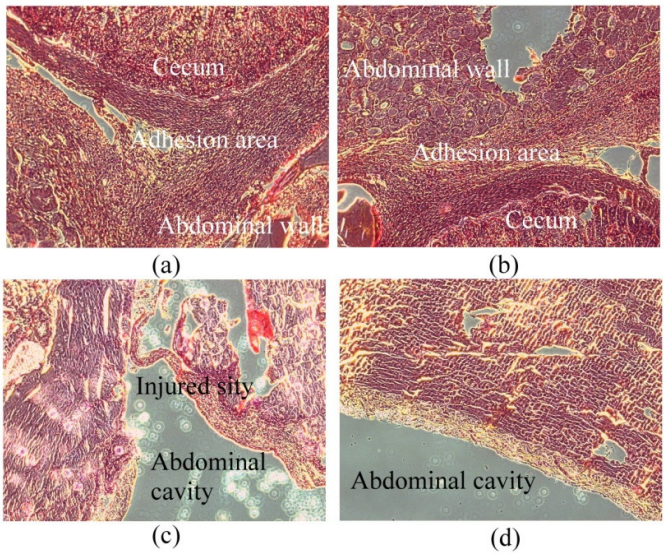

Fig.7. Histological observation of the wound site in the operated rats 3 and 7 days after surgery：(a,b)control group and (c,d) treated with gellan gum-cin film. Thin sections were stained with H-E(100 x).

3.6. Quantitative analysis of the inflammatory cells

We also assessed the number of peritoneal fluid neutrophils to evaluate whether the gellan gum-cin film had an anti-inflammatory capacity. The results showed that on the 3rd and 7th days following surgery, the number of neutrophils in the control group was $2.0\pm 0.6 \times 10^5$ and $1.7\pm 0.5 \times 10^5$ cells/ml, respectively, whereas the number of neutrophils in the experimental group was $1.1\pm 0.2 \times 10^5$ and $0.9\pm 0.5 \times 10^5$ cells/ml,

respectively. For all test groups, the number of neutrophils reached a maximum within the first 3 days after surgery and then gradually decreased over the 7-day period of observation. On the 3rd day after surgery, the number of neutrophils in the control group was 1.81 (P-value 0.046) times that of the experimental group. On the 7th day after surgery, the number of neutrophils in the control group was 1.88 (P-value 0.0008) times that of the experimental group. Neutrophils are the predominant inflammatory cell type found in a wound during the first 7 days after injury. After injury, the normal healing process leads to inflammation and some scarring, which patches the damaged tissue. However, if an injury is not properly addressed, inflammation and scar tissue (adhesion fibrosis) can become more severe, leading to the beginning of a chronic injury cycle (Delavary et al., 2011). Our results demonstrated that a gellan gum-cin film could effectively inhibit inflammation in rats. In this study, gellan gum film plays a role not only as a physical barrier for the separation of wounded tissues after surgery but also as an anti-inflammatory drug carrier.

Conclusion

Various types of biodegradable films based on polysaccharide have been developed for anti-adhesion. Polysaccharides have high amounts of free carboxyl groups. At neutral pH, these polysaccharides and living cells are negatively charged. Stronger negative charges on the polysaccharide film surface provide long-range electrostatic repulsion, which can prevent the rapid adhesion of cells (Vitte et al., 2004). In addition, the details of cell-polysaccharide interaction remain largely uncharacterized. In this study, we have developed a new method to cross-link gellan gum using the cinnamate group as the cross-linker and designed a novel anti-adhesion film base on microbial polysaccharide gellan gum. The results of the in vitro characterization and in vivo evaluation of post-surgery anti-adhesion capability demonstrated that gellan gum-cin film has great potential for future use in clinical applications.

References

1. Allen, N. S., Mallon, D., Timms, A., Green, A. W., Catalina, F. (1993). Synthesis and spectroscopic properties of novel cinnamate derivatives of thioxanthone: photocuring activity versus photodimerization. *Polymer*, 34 (11), 2401-2406.
2. Ballabeni, V., Tognolini, M., Giorgio, C., Bertoni, S., Bruni, R., Barocelli, E. (2010). Ocotea quixos Lam. essential oil: In vitro and in vivo investigation on its anti-inflammatory properties. *Fitoterapia*, 81 (4), 289-295.

3. Chang, S. J., Kuo, S. M., Liu, W. T., Niu, C. G., Lee, M. W., & Wu, C. S. (2010). Gellan gum films for effective guided bone regeneration. *Journal of Medical and Biological Engineering*, 30, 99–103.

4. Coutinho, D. F., Sant, S.V., Shin, H. Oliveira, J. T., Gomes, M.E., Neves, N. M., Khademhosseini, A., Reis, R. L. (2010). Modified gellan gum hydrogels with tunable physical and mechanical properties. *Biomaterials*, 31 (29), 7494-7502.

5. Delavary, B. M., van der Veer, W. M., van Egmond, M., Niessen, F. B., Beelen, R. H. J. (2011). Macrophages in skin injury and repair . *Immunobiology*, 216 (7), 753-762.

6. Dong, C. M., Wu, X., Caves, J., Rele, S. S., Thomas, B. S., Chaik, E. L. (2005). Photomediated crosslinking of C6-cinnamate derivatized type I collagen. *Biomaterials*, 26 (18), 4041-4049.

7. Francisco, R. M., Maria Jose, S. R., Pedro Antonio, G. R. (2007). Photocuring of cinnamic carbohydrate esters: Controlling the reaction by monocinnamoylated derivatives. *Carbohydrate Polymers*, 68, 424-432.

8. Ichibouji, T., Miyazaki, T., Ishida, E., Sugino, A., Ohtsuki, C. (2009). Apatite mineralization abilities and mechanical properties of covalently cross-linked pectin hydrogrls. *Materials Science and Engineering ：C*, 29(6), 1765-1769.

9. Jansson, P. E., Lindberg, B. & Sandford, P. A. (1983). Structural studies of gellan gum an extracellular polysaccharide elaborated by Pseudomonas elodea. *Carbohydrate Polymers*, 124, 135–139.

10. Lee, M. W., Chen, H. J., & Tsao, S. W. (2010). Preparation, characterization and biological properties of Gellan gum films with 1-ethyl-3-(3-dimethylaminopropyl) carbodiimide cross-linker. *Carbohydrate Polymers*, 82(3), 920–926.

11. Mathew, S., Abraham, T. E. (2008). Characterisation of ferulic acid incorporated starch–chitosan blend films. *Food Hydrocolloids*, 22 (5), 826-835.

12. Nagasawa, N., Yagi, T., Kume, T., Yoshii, F. (2004). Radiation crosslinking of carboxymethyl starch. *Carbohydrate Polymers*, 58 (2), 109-113.

13. Nagata, M., Inaki, K. (2009). Synthesis and characterization of photocrosslinkable poly(l -lactide)s with a pendent cinnamate group. *European Polymer Journal*, 45 (4), 1111-1117.

14. Oliveira, J. T., Martins, L., Picciochi, R., Malafaya, P. B., Sousa, R. A., Neves, N. M., Mano, J. F., Reis, R. L. (2010). Gellan gum: a new biomaterial for cartilage tissue engineering applications. *Journal of Biomedical Materials Research Part A*. 93(3), 852-863.

15. O'Neil, M. A., Selvendran, R. R., & Morris, V. J. (1983). Structure of the acidic extracellular gelling polysaccharide produced by Pseudomonas elodea. *Carbohydrate*, 124, 123-133.
16. Oudshoorn, M. H. M., Rissmann, R., Bouwstra, J. A., Hennink, W. E. (2007). Synthesis of methacrylated hyaluronic acid with tailored degree of substitution. *Polymer*, 48 (7), 1915-1920.
17. Peng, H. H., Chen, J. W., Yang, T. P., Kuo, C. F., Wang, Y. J., Lee, M. W. (2011). Polygalacturonic acid hydrogel with short-chain hyaluronate cross-linker to prevent postoperative adhesion. *Journal of Bioactive and Compatible Polymers*, 26 (6), 552-564.
18. Powell, H. M., Boyce, S. T. (2006). EDC cross-linking improves skin substitute strength and stability. *Biomaterials*, 27(34), 5821-5827.
19. Robertson, D., Lefebvre, G., Leyland, N., Wolfman, W., Allaire, C., Awadalla, A., Best, C., Contestabile, E., Dunn, S., Heywood, M., Leroux, N., Potestio, F., Rittenberg, D., Senikas, V., Soucy, R., Singh, S. (2010). Adhesion prevention in gynaecological surgery. *Journal of Obstetrics and Gynaecology Canada*, 32(6), 598-608.
20. Silva-Correia, J., Oliveira, J. M., Caridade, S. G., Oliveira, J.T., Sousa, R. A., Mano, J. F., Reis, R. L. (2011). Gellan gum-based hydrogels for intervertebral disc tissue-engineering applications. *Journal of Tissue Engineering Regenerative Medicine*, 5(6), 97-107.
21. Sudhamani, S. R., Prasad, M. S., & Udaya Sankar, K. (2003). DSC and FTIR studies on gellan and polyvinyl alcohol (PVA) blend films. *Food Hydrocolloid*, 17, 245–250.
22. Sung, S. J., Cho, K. Y., Yoo, J. H., Kim, W. S., Chang, H. S., Cho, I., Park, J. K. (2004). Dimerization behavior of cinnamate group attached to flexible polymer backbone and its effect on the molecular orientation. *Chemical Physics Letters*, 394 (4-6), 238-243.
23. Vijayabaskar, V., Tikku, V. K., Bhowmick, & Anil, K. (2006). Electron beam modification and crosslinking: Influence of nitrile and carboxyl contents and level of unsaturation on structure and properties of nitrile rubber. *Radiation Physics and Chemistry*, 75, 779–792.
24. Vitte, J., Benoliel, A. M., Pierres, A., Bongrand, P. (2004). Is there a predictable relationship between surface physical-chemical properties and cell behaviour at the interface? *European cells & materials*, 7, 52-63.
25. Watanabe, S., Ichimura, K., Suda, Y. (1986). Preparation and reactions of polymers having 1-aroyl-2-(3-pyridyl)ethylenes as photosensitive groups. *Journal of Applied Polymer Science*, 32 (3), 4127-4135.

26. Zuhlke, H. V., Lorenz, E. M., Savvas, V. (1990). Pathophysiology and classification of adhesions. *Langenbecks Archiv fur Chirurgie. Supplement II, Verhandlungen der Deutschen Gesellschaft fur Chirurgie*, 190, 1009-1016.

主題四：Preparation, characterization and biological properties of Gellan gum films with 1-ethyl-3-(3-dimethylaminopropyl)carbodiimide crosslinker

Abstract

Gellan gum (GG) is an exopolysaccharide produced by *Sphingomonas elodea*. To develop a medical application for GG, in this study we prepared 26 μm thick films of GG reacted with 1-ethyl-3-(3-dimethylaminopropyl)carbodiimide (EDC) in 40% ethanol to obtain a cross-linked film (GG40) with 73% gel content and 52.4 MPa tensile strength. In vitro biocompatibility tests, GG40 film exhibit nontoxic effects for L929 cells and inhibit absorption and activation of platelets. When implanted into rat subcutaneous tissue, the GG40 film caused minor inflammation in the early postoperative period. The results indicate that the effects of GG40 film on wound healing, wound size reduction (%) and collagen content are higher than those found in commercial products (Duoderm). Therefore, we conclude that the GG film developed in this study has potential for future use in surgical applications.

1. Introduction

Gellan gum (GG) is an exopolysaccharide (EPS), also known as polysaccharide S-60, which is a gelling agent produced by a non-pathogenic strain of *Sphingomonas elodea* ATCC 31461 (Pollock, 1993). Natural GG is a linear electronegative EPS. The main chain of GG consists of four repeating carbohydrates, which includes two D-glucose carbohydrates, one L-rhamnose, and one D-glucuronic acid. In its natural form, GG has two acyl-substituted positions (O-acetate and L-glycerate), which separately connect to the C-6 and C-3 positions of the same glucose molecule. On average, each repeated unit of the main chain has 1 glycerate and 0.5 acetate molecules (Jansson, Lindberg, and Standford, 1983; Jay et al., 1998). GG has the ability to form gel in the presence of cations, but the presence of acetyl groups can interfere with the bonding ability of the ions. The average molecular weight of GG is approximately 500 kDa (Bemiller, 1996).

GG is a food additive approved by the FDA. Although it is extensively used in the foodstuff industry, GG has rarely been investigated for biomedical applications, except for use in drug delivery. Beginning in 2008, Wang C. et al used modified GG to cultivate human dermalfibroblasts and human fetal osteoblasts. GG has also

become an innovative material in applications of tissue engineering. Several advantages of GG are listed here. 1. The GG with heat and acid stability, adjustable elasticity and hardness, and high transmittance (Rinaudo, 2004), which allows the material to easily change form and accommodate many different applications. 2. It has an active reaction group that is suitable for chemical modification, which allows its use in preparing conjugates with molecules of biological activity to increase its range of applications in medical research. 3. GG is a bacterial exopolysaccharide, prepared commercially by aerobic submerged fermentation from *Sphingomonas elodea.* This process, or the associated purification steps, is not complex (Fialho et al., 2008) and is suitable for development for use in the industry.

The goal of this study is to develop GG for surgical applications by preparing and characterizing a water-insoluble GG film. In addition, this study evaluates the in-vitro and in-vivo biocompatibility and effects of cross-linked GG film on wound healing.

2. Methods

2.1. Preparation of GG films

GG of 0.3 g (Sigma G1910) was dissolved in 30 ml de-ionzed water (DDW) and heated at 85-90℃ until it became a transparent solution. The solution was then poured onto a glass dish (diameter 10 cm) and evaporated at 37℃, 1 atm for 3 days to obtain the dry film (GG film). The GG films were then cross-linked by immersing them into an EtOH(ethanol)/DDW solution containing 15 mM 1-ethyl-3-(3-dimethylaminopropyl)carbodiimide (EDC, sigma 1769), for 24h at room temperature. To study the effects of the EtOH composition on the EDC cross-linking of the GG, EtOH was diluted in DDW to yield an EtOH/DDW (v/v%) solution. This study used 0%, 20%, 30%, 40%, 50%, 60%, 70%, 80%, 90% and 100% EtOH/DDW. The cross-linked films (denoted as GG0, GG20, GG30, GG40, GG50, GG60, GG70, GG80, GG90 and GG100) were washed with 95% ethanol three times to remove any non-reacted residual EDC and then dried at room temperature (Lee et al., 2005).

2.2. Characterizations of the GG films

An electrical thickness tester (Mitutoyo, MDC-25 SB) was used to measure the thickness of the GG films. We used the FTIR-L396A (Perkin-Elmer) to analyze the properties of the chemical functional groups of the GG films. The analysis of the gel content of the GG films was performed as follows. After drying, we weighed the cross-linked film (W1) and then swelled it in DDW at 37℃ for 24 h. After removing the wet film from the solution, it was dried in a vacuum oven for 12 h at 60℃ and then weighed again (W2). The following equation was then used to calculate the gel content of the film (Kenji and Ilada, 1997):

Gel content (%) = （W2/W1） x 100%

2.3. Mechanical property measurement

GG films were cut into 1 cm × 5 cm pieces (Kuo, 2009). We then used the H1-KS testing machine (Tinius Olsen) with a crosshead speed of 5 mm/min to measure the mechanical properties of the GG films and to automatically record the mechanical parameters.

2.4. Platelet absorption test

Blood drawn from a human body was used to prepare the platelet concentrate. We then prepared and filtered Hepes-Tyrode buffer solution using a 0.45 μm filter. The GG films were then sterilized with 75% ethanol for 24 hr The sterilized films were placed on a 24-well bottom and added with Hepes-Tyrode buffer solution (1 ml) at 37℃ for 15 min. After aspiration of the solution, each well was added with platelet concentrate 1ml (density $2.9x10^5$/μl), and incubated at 37℃ for 120 minutes. The Automatic Hematology Analyzer (Sysmes KX-21) was then used to determine the number of platelet absorbed on the films. In addition, the SEM (positive control: glass) was used to observe the morphology of the platelets absorbed on the GG films (Ishihara et al., 2004).

2.5. MTT assay

The preparation and placement of 11 mm diameter polymeric discs in the bottom of each well of a 48-well tissue-culture plate was used to determine the cell adhesion and the cell growth on the GG films (GG40). We added fibroblast (L-929) cells to the plate with a population of $3×10^4$ cells for each well and incubated them at 37℃. As a positive control, the cells were plated onto 48-well tissue-culture plates (NUNC, Roskilde Denmark). By changing the culture medium, we determined the cell number on each synthetic film after 24, 48, and 72 hr of cell seeding by implementing the MTT test. Five independent measurements were conducted for each experimental value (Lee et al., 2005).

2.6. *In-vivo* biocompatibility (subcutaneous implantation)

The purpose of the experiment was to examine the immune compatibilities of GG in an organism. GG40 and Hyaluronic acid (HA) film (control group) were cut into 1.5x1.5 cm^2 pieces (Ramire et al., 2005). HA as the control group is because it possesses good compatibility (Kenji and Ilada, 1997). The following experimental procedures were then used. SD-rats (male, 250~300g) were etherized with 4% trichloroacetaldehyde monohydrate (1mg/ml). We shaved the skin of the animal and

disinfected it using iodophor. The polymeric film was implanted in the back of the specimen. The rats were sacrificed on the 3rd, 14th and 30th days after the operation. Five mm wedged tissue were cut from the wound, including the implanted film, granulation tissue, connective tissue, and inferior muscle. The tissues were processed using the standard procedure for histological examinations and their thin sections were examined after staining with Hematoxylin–Eosin (H&E). The animal experiments in this study were approved by the Chung-Shan Medical University Experimental Animal Center.

2.7. Experiment on wound healing

To develop the medical application of GG as a biomedical material, this study was conducted to evaluate the effect of GG on the wound healing process on laboratory rats. Epithelium with an area of 2x2 cm^2 was cut from the backs of etherized SD rats (male, 250~300g). The wound was then treated by applying either commercial Duoderm (control group) or GG40 film (experimental group) and bandaged with gauze. Duoderm is a synthetic dressing, with a bilaminate structure with an outer layer of polyurethane foam and an inner layer that is contain sodium carboxymethylcellulose and gelatin (Leicht et al., 1991). Duoderm is the most commonly used dressing in wound care.

Following the sacrifice of the rats after the 5th, 15th, and 24th days, we measured the sizes of the wound area. Reductions in wound size were used as an indicator of wound healing (n=4). The following equation was used to determine the reduction in wound size (Yang et al., 2008):

$$\text{Wound size reduction } (\%) = A_0\text{-}A_t/A_0$$

where A_0 and A_t are the initial wound area and wound area after time interval ‘t’, respectively. Photographs of the wounds were used for measurement purposes using image analysis software (Image J). Then removed the wound tissue for sectioning (2-3 μm thick) and observed the histology around the wound using H&E staining. In addition, the Masson's trichrome stain was used to observe the formation and distribution of collagen on the wounds (collagen is stained blue). For the relative quantization of collagen, Image J software was used to measure the color values of the blue stain. First, an inverted light microscope (Axiovert 200) was used to record the regenerated tissues using the 20X object lens. The recording position covered all the regenerated tissues. Then, an analysis of the blue color value of each picture was used to determine the average value. A light color and low collagen content indicated a high color value.

2.8. Statistical analysis

Each of the experiments was repeated at least four times, and the values were expressed as means ± standard deviations. For comparison between two groups of data, the Student's t-test was performed. Differences were considered to be statistically significant at $P<0.05$.

3. Results and discussion

3.1. Gel content of cross-linked GG film

EDC is the most widely used reagent for chemical cross-linking. To solve the problem of EDC hydrolysis in water, previous studies (Kwangwoo, Tsuyoshi, Seiichi and Akio, 2010; Montalbetti and Falque, 2005) have suggested using a mixture of EtOH/DDW as the reaction solvent. Fig.1 shows the gel content of GG films cross-linked in various concentrations of ethanol with 15 mM EDC for 24 hrs. In the control group (without EtOH), the gel content of GG film was found to be only 15±2.0% and showed a poor degree of cross-linking. In 40% ethanol (i.e. GG40 film), the gel content was found to be highest 73±2.6%. In this system the increase of cross-linking degree was not proportional to the ethanol content. This is due to the polymer chain difficulty of the hydrophilic GG to extend in organic solvents, which reduces its reactivity. An ethanol content of 40% was found to be the most suitable condition for cross-linked GG.

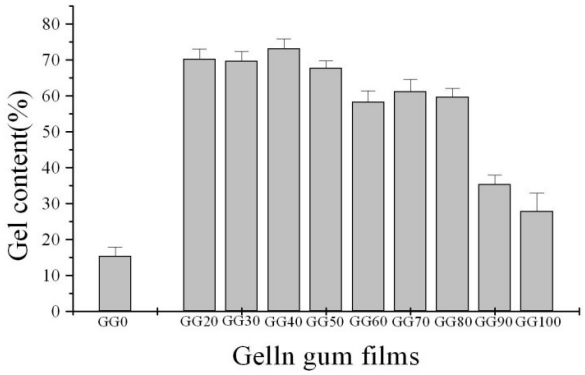

Fig.1. The gel content of GG films cross-linked in various concentrations of ethanol with 15 mM EDC for 24 hrs.

3.2. Mechanical properties of GG film

Fig.2 shows the tensile strength of GG films cross-linked in various concentrations of ethanol with 15 mM EDC for 24 hrs. The average thickness of films was 26±3 μm. The results indicate that GG30, GG40, and GG50 have high tensile strengths of 45.3±9.6 MPa, 52.4±2.3 MPa, and 43.2±11.1 MPa, respectively. Previous

studies demonstrate that the tensile strength of a polymer is closely correlated to the density of cross-linking (Sen, Majumder and Bhowmick, 1999; Vijayabaskar et al., 2006). At lower cross-link density, the tensile strength increases with an increase in the cross-link density. However, at higher cross-link density, the segments of macromolecules become immobile, due to which the system becomes stiff and shows a decrease in elasticity. Based on gel content and mechanical property measurement, GG in 40% ethanol optimizes the cross-linked environment. In summary, with regards to mechanical property, GG40 is suitable for potential application as wound dressing, which has typical values in the range of 2.5-16 MPa (Ezequiel et al., 2009). Therefore, in this study we have selected GG40 as the substrate of choice for evaluating biocompatibility and effects on wound healing.

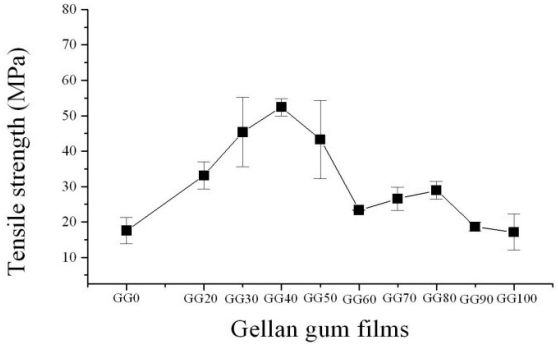

Fig.2. The tensile strength of GG films cross-linked in various concentrations of ethanol with 15 mM EDC for 24 hrs.

3.3. FTIR characterization of GG film

Fig.3A and Fig.3B show FTIR spectrograms of non-cross-linked GG and GG40 films. Fig.3A shows the assignment of the absorption band at 3291 cm^{-1} for stretching the –OH groups in GG. The band at 2921 cm^{-1} is due to the stretching vibrations of the $–CH_2$ group (Xu et al., 2007; Agihortri, Jawalkar and Aminabhavi, 2006), whereas those appearing at 1020 cm^{-1} and 1149 cm^{-1} are due to ethereal and hydroxylic C-O stretching. The peaks at 1605 cm^{-1} and 1405 cm^{-1} can be assigned to the characteristic absorption band of carboxyl in non-crosslink GG. The bending vibration of C-H appears at 888 cm^{-1} (Alupi et al., 2006; Sudhamani, Prasad and Udady Sankar, 2003). Fig.3B shows both the FTIR spectrogram of GG40 film and a new absorption peak at 1720 cm^{-1} (Lee et al., 2005). This indicates that carboxyl grouped on β-D-glucuronic acid (Glcp A) of GG can generate an ester bond with -OH groups. It also causes the absorption peak of the -OH groups to shift to a higher wave number - 3347 cm^{-1}, and the C-O stretching to shift from 1020 cm^{-1} to 1027 cm^{-1}. However, the absorption peak

of $–CH_2$ groups shows no shift both before and after cross-linking. These data indicate that the new absorption peak is not caused by residual EDC and confirms that the cross-linking reaction was successful.

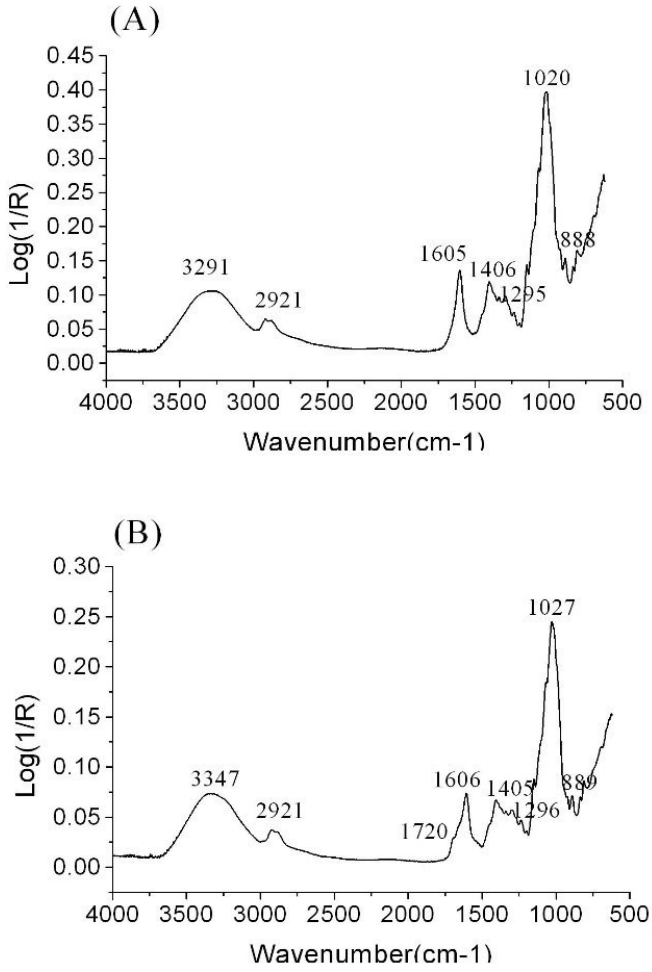

Fig.3. FTIR spectra of non-crosslinked GG film (A) and crosslinked GG film (B).

3.4. Platelet adhesion

Measurements performed using an Automatic Hematology Analyzer indicated that there was a large amount of platelet absorption in the positive control group ($6x10^4/\mu L$). However, when the platelets encountered the GG40 film after 120 min, the amount of absorption on the film was lower than $1x10^3/\mu L$ (the minimum limit measurable by the Analyzer). We used SEM to observe the surface of the GG40 film. The average number of absorbed platelets under each view (7500X) was found to be less than 1 (Fig.4B). The SEM image was also used to observe the morphology of platelets absorbed on the base material due to their activation in the positive control

group (glass). Obvious pseudo pods were observed on the platelets (Fig.4A) (Mao et al., 2004). The platelets absorbed on the surface of the GG40 film were round in shape and without pseudo pods (Fig.4B). The results confirm that GG40 film can resist the absorption of platelets and is a type of inert material for them.

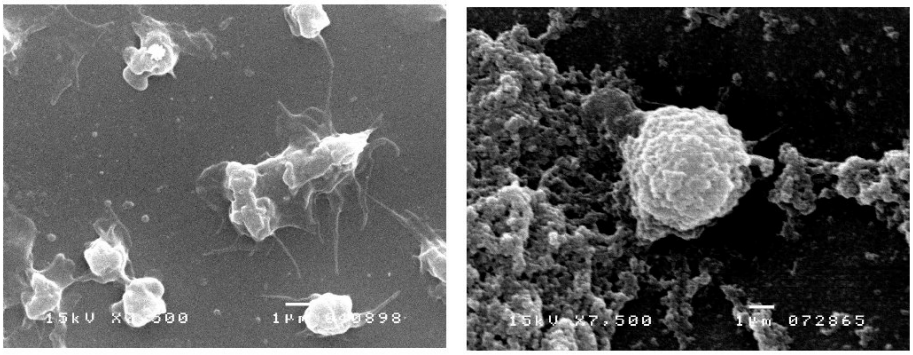

(A) (B)

Fig.4. The morphology of platelets absorbed on the surface of Glass (A) and GG40 (B) (SEM 7500X).

3.5. Attachment and growth of L929 fibroblast cells on GG film

As an *in-vitro* screening test for the adhesion capability of GG film to fibroblast, we inoculated the L929 fibroblast cells onto the GG40 film, cultured them for designated periods, and evaluated the cell viability with MTT assay. Fig.5 shows the results of this MTT test. In the 24 hr period following cell seeding, an absorbance unit of only 0.6 was displayed by the viable cells on the GG40 film as compared with the 1.1 units of cells grown on cultured flasks. This indicates that GG40 was able to inhibit cell adhesion attributable to the negatively charged surface (Lee et al., 2005). However, once the cells attached to the surfaces of the GG40 film or the flask, the attached cells proliferated at approximately equal rates, as indicated by the similarity in slope of increasing absorbance. This implies that GG40 film disfavored cell adhesion and exhibited a nontoxic effect on the attached cell.

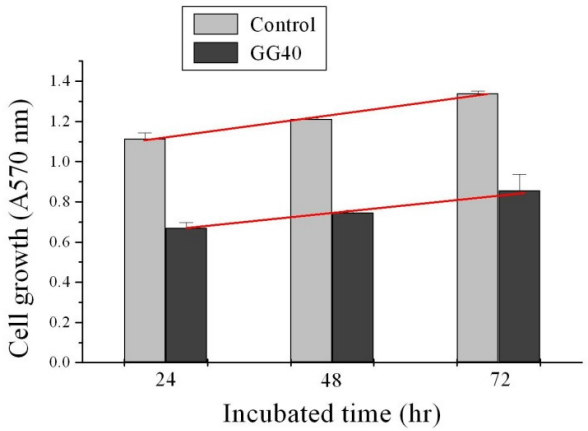

Fig.5. Viability of L929 cells after 24hr, 48hr, and 72hr exposures to GG40 (n=5,results are given as mean values, bars represent standard deviation).

3.6. *In-vivo* biocompatibility

Researcher implanted HA film (positive control) and GG40 films in the SD-rats' subcutaneous tissue to evaluate inflammation reaction. In the positive control, histological examination showed that there were inflammatory cells in contact between the material and the tissue on the 3 days after implanting (Fig.6A) (Fernandez-Cossio et al., 2007; Fulzele, Satturwar and Dorle, 2007). On the 14 days after implanting, there were no residual materials in the gross examination. Examination of histology (Fig.6B) found that there was no inflammation of cells, which indicates that HA film does not cause chronic inflammation. After we had implanted GG40 films for 3 days and 14 days, histological examination showed the presence of Neutrophil (N) and Macrophage (M) (Fig.6C, Fig.6D). Neutrophil is an indicator of acute inflammation, and Macrophage is an indicator of chronic inflammation (Wang et al., 2006; Kweon, Song and Park, 2003). This proves that GG40 film may lead to both acute and chronic inflammation. Continuous follow-up studies of the inflammation caused by the GG40 film showed that the histological section (Fig.6E) had only a few macrophages from the implanted materials existing after 1 month. In terms of visual observations, residual materials could be seen after the GG40 film had been implanted for 1 month. This suggests that long-term follow-ups are important. In addition to inflammation, histological section showed subcutaneous tissue with no fibrosis, stromal reaction, or vaccularity (Macleod et al., 2005). Based on the results, it can be concluded that GG40 film demonstrate good in-vivo biocompatibility.

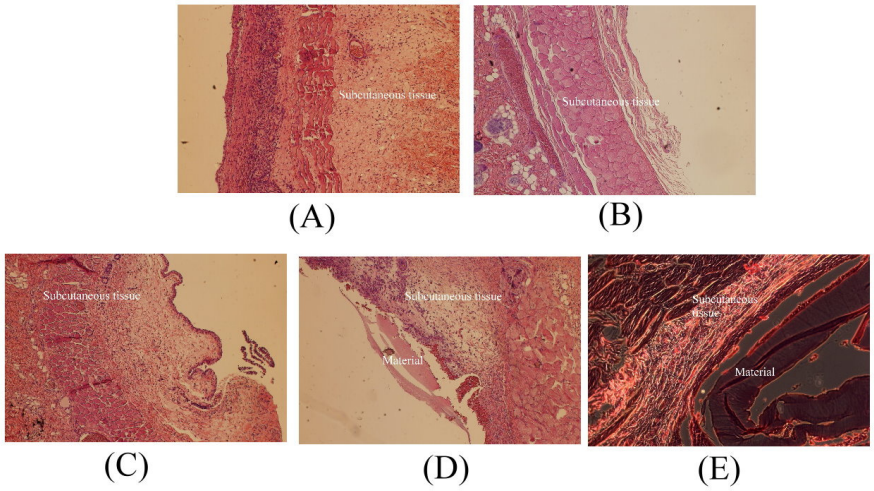

Fig.6. Micrograph of rat subcutaneous tissue response to Hyaluronic aic (HA, control) and GG40 film (HE stain x200) (A) HA-3 days (B) HA-14 days (C) GG40-3 days (D) GG40-14 days (E) GG40-30 days after surgery.

3.7. *In-vivo* wound healing

3.7.1 Gross examination

In this study, Duoderm and GG40 film were placed on the SD-rat wound sites 5, 15, and 24 days after surgery for observation in macro vision. After 5 days, the dressing and the wound in the control group showed severe adhesion, and hemorrhage occurred upon removal of the dressing (Fig.7A). In the GG40 group, we observed a healthy, clean wound, pink and red in color, during the healing process. In addition, the GG40 film adhered to the wound only slightly, and we were able to remove it from the wound surface without causing further trauma (Fig.7D). After 15 days, it was difficult to separate the Duoderm from the tissue, which resulted in considerable tissue bleeding during removal of the dressing. As a result, the wound healing process was prolonged. Nevertheless, for GG40 dressings, the wound was kept moist and no signs of inflammation and infection were observed (Fig.7B and 7E). In a previous study, Winter reported that the epithelialization process can be accelerated if the wound is kept moist (Winter, 1962; Winter and Scale, 1963). The epidermal cells migrate more easily over a moist wound surface than under a scab in dry wounds (Yang et al., 2010). After twenty-four days, for both Duoderm and GG40 dressings, most wound tissues repaired themselves with no obvious residual scar tissue.

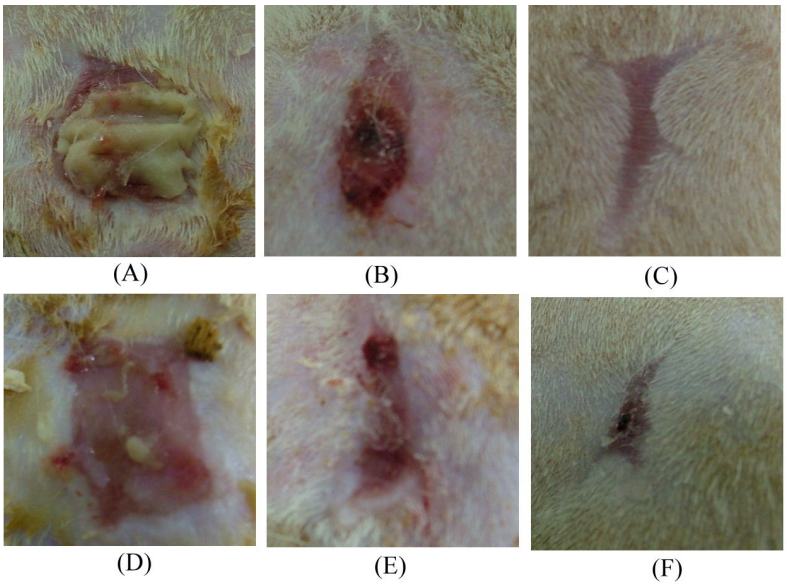

Fig.7. Representative photographs of macroscopic appearance of a 2x2 cm^2 wound excised on rat, control wounds at 5 (A), 15 (B) and 24 days (C), and GG40 film wounds at 5 (D), 15 (E) and 24 days (F) after surgery.

This study calculated the reduction in the wound defect area by measuring the wound area size before and after fixed intervals of time (Balakrishnan et al., 2005). In the control group, 5, 15, and 24 days after surgery, the wound size reduction (%) was 31±7%, 45±9%, and 89±3%, respectively. In the experimental group, 5, 15, and 24 days after surgery, the wound size reduction (%) was 34±3%, 54±11%, and 88±3%, respectively. The wound size reduction in the control and experimental group at 15 days showed statistically significant differences ($P<0.05$). On the 24 days after the operation, the difference in wound size reduction between the two groups was not statistically significant ($P>0.05$). Based on the above results, it can be conclude that in the first few days after operation the effects of GG40 film in promoting healing are superior to those of Duoderm.

3.7.2 Histological examination

Rat skin tissue includes several different parts, such as the epidermis, dermis, musculoautaneous layer, and subcutaneous tissue. The histological sections showed a regenerated tissue structure and inflammation at the epidermis and dermis layers (Ong et al., 2008; Li et al., 2008). In the control group, the epidermis had regenerated on the 5 days after surgery (Masson's trichroma stain, Fig.8A). However, some tissues had separated because the structure was incomplete. The GG40-film-treated group (Fig.8D) exhibited a deeply stained epidermis color similar to that of the original tissue, which indicates that the structure was more compact. In addition, inflammatory

cells were visible in the regenerated dermis, the control group and the test group, which suggests that inflammation occurred. According to literature (Balakrishnan et al., 2005), inflammation is inevitable in the early stages of a wound because dressing is a foreign matter. Additionally, the regenerated dermis in the experimental group showed many fibrous extracellular ground substances. It is evident the regeneration of tissues occurred faster in the experimental group. Again, both groups displayed regenerated blood vessels, and no bacterial colonies were found in either group. On the 15 days after surgery, the generated epidermis in the control group (Fig.8B) was still not compact, and the regenerated dermis showed round nucleus cells. In the test group (Fig.8E), the cells in the dermis were primarily fibrous. Regardless of the group, integration occurred at the junction between regenerated and original tissues and exhibited a higher level of tissue healing. On the 24 days after surgery, the histological sections (Fig.8C, Fig.8F) showed that the amount of regenerated tissue was similar between the control and test group. This length of time is sufficient to allow the majority of wound tissues to repair and explains the similarities between the two groups.

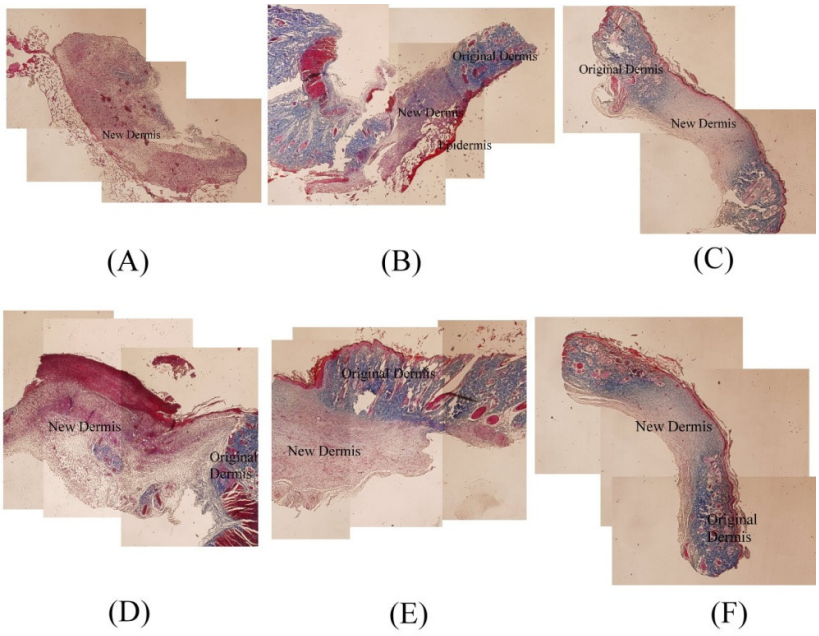

Fig.8. Micrograph of wound re-epithelialization in control group 5 (A), 15 (B) and 24 days (C), and GG40 film group 5 (D), 15 (E) and 24 days (F) after surgery (Masson's trichrome stain x100).

The extracellular ground substances of the skin tissues primarily contain type 1 collagen. To determine the distribution of extracellular ground substances of the regenerated tissues, we utilized the Masson's trichrome stain to stain the collagen (Li

et al., 2008). The basis for the relative quantity of collagen is the blue color value of the tissue sections (if blue is stronger, the value is lower). In the control group, 5, 15, and 24 days after surgery, the color value of blue was 110±16, 91±12, and 75±7, respectively. In the experimental group, 5, 15, and 24 days after surgery, the color value of blue was 108±22, 88±6, and 70±3, respectively. The data indicate that color value decreases with increase in time in both the control and experimental groups. This also indicates that the amount of collagen secreted increases with increase in time. Five and fifteen days after the surgery, the color values between the two groups showed no statistically significant difference ($P>0.05$). Twenty-four days after the surgery, the color value of the test group was lower than that of the control group ($P<0.05$), which suggests that the test group had larger amounts of collagen secretion. This result confirms that GG40 film is a better option than the commercially used Duoderm during the wound healing process. In addition, the results could also be used to estimate the differences between regenerated collagen and collagen of the original tissues. The collagen of the original tissues was blue (color value 108±5), whereas the regenerated collagen was bluish grey. The collagen of the original tissues was loosely distributed whereas the regenerated collagen was more compact. Past studies have reported that inflammation reaction can delay the regeneration of tissues (Jones, Edwards and Thomas, 2004). In this study, GG40 film showed a high level of biocompatibility and excellent physical properties, which could help promote wound healing.

4. Conclusion

GG is one of many microbial polysaccharides used in drug delivery, tissue engineering, and in the food industry, but not in surgical applications such as wound healing and dressing. Therefore, this study prepared water-insoluble GG films and studied their characterization and biological properties to expand future medical applications. EDC can activate the galacturonic acid residues contained within the GG molecule. To prevent EDC hydrolysis in water, we applied ethanol as the reaction solvent, with results suggesting that highest gel content was observed when the GG was cross-linked in 40% ethanol. From the FTIR analysis, the mechanism of EDC cross-linking in the GG was the condensation reaction between the carboxyl and hydroxyl group. Because polysaccharide films normally possess poor mechanical strength, the results obtained in this study indicate that GG40 film is suitable for potential applications in skin replacement. With respect to in-vitro biocompatibility, MTT assay revealed that GG40 is compatible with both L929 fibroblast cells and blood. With respect to in-vivo biocompatibility, subcutaneous implantation showed that GG40 caused slight inflammation in the first few days after operation, but no

fibrosis or stromal reaction in either long-term or short-term implantation. In the wound healing test, GG40 film demonstrated good physical properties and biocompatibility, and proved to be capable of accelerating wound repair. In conclusion, EDC cross-linked GG film have great potential for future use in clinical applications.

Reference

1. Agnihotri, S. A., Jawalkar, S. S., Aminabhavi, T. M. (2006). Controlled release of cephalexin through gellan gum beads: Effect of formulation parameters on entrapment efficiency, size, and drug release. *European Journal of Pharmaceutics and Biopharmaceutics*, 63, 249-261.
2. Alupei, I. C., Popa, M., Bejenariu, A., Vasiliu, S., Alupei, V. (2006). Composite membranes based on gellan and poly(*N*-vinylimidazole). Synthesis and characterization. *European Polymer Journal*, 42, 908-916.
3. Balakrishnan, B., Mohanty, M., Umashankar, P. R., Jayakrishnan, A. (2005). Evaluation of an in situ forming hydrogel wound dressing based on oxidized alginate and gelatin. *Biomaterials*, 26, 6335-6342.
4. Bemiller, J. N. (1996). Structure-property relationships of water-soluble polysaccharides. *Journal of Applied Glycoscience*, 43, 377-384.
5. Fernández-Cossío, S., León-Mateos, A., Sampedro, F. G., Oreja, M. T. (2007). Biocompatibility of agarose gel as a dermal filler: histologic evaluation of subcutaneous implants. *Plastic & Reconstructive Surgery*, 120, 1161-1169.
6. Fialho A. M., Moreira L. M., Granja A. T., Popescu A. O., Hoffmann K., Sá-correia I. (2008). Occurrence, production, and applications of gellan: current state and perspectives. *Applied Microbiology and Biotechnology*, 79, 889-900.
7. Fulzele, S. V., Satturwar, P. M., Dorle, A. K. (2007). Novel biopolymers as implant matrix for the delivery of ciprofloxacin: biocompatibility, degradation, and in vitro antibiotic release. *Journal of Pharmaceutical Sciences*, 96, 132-144.
8. Hamcerencu, M., Desbrieres, J., Khoukh, A., Popa, M., Riess, G. (2008). Synthesis and characterization of new unsaturated esters of Gellan Gum. *Carbohydrate Polymers*, 71, 92-100.
9. Ishihara, K., Nishiuchi, D., Watanabe, J., Iwasaki, Y. (2004). Polyethylene/phospholipid polymer alloy as an alternative to poly(vinylchloride)-based materials. *Biomaterials*, 25, 1115-1122.
10. Jansson, P. E., Lindberg, B., Sandford, P. A. (1983). Structural studies of gellan gum, an extracellular polysaccharide elaborated by Pseudomonas elodea. *Carbohydrate Research*, 124, 135-139.
11. Jay, A. J., I. J. Colquhoun, M. J. Ridout, G. J. Brownsey, V. J. Morris, A. M.

Fialho, J. H. Leitão, and I. Sá- Correia. (1998). Analysis of structure and function of gellans with different substitution patterns. *Carbohydrate Polymers*, 35, 179-188.

12. Jones, S. G., Edwards, R., Thomas, D. W. (2004). Inflammation and wound healing:the role of bacterials in the immune-regulation of wound healing. T*he International Journal of Lower Extremity Wounds*, 3, 201-208.
13. Kenji, I., Ikada, Y. (1997). Preparation of cross-linked hyaluronic acid films of low water content. *Biomaterials*, 18, 189-195.
14. Kuo, S. M., Chang, S. J., Niu, C. C., Lan, C. W., Chen, T. W., Yang, C. Z. (2009). Guided tissue regeneration with use of β-TCP/chitosan composite membrane. *Journal of Applied Polymer Science ： Applied Polymer Symposium*, 112, 3127-3134.
15. Kwangwoo, N., Tsuyoshi, K., Seiichi, F., Akio, K. (2010). Preparation of a collagen/polymer hybrid gel designed for tissue membranes. Part I: Controlling the polymer-collagen cross-linking process using an ethanol/water co-solvent. *Acta Biomaterialia*, 6, 403-408.
16. Kweon, D. K., Song, S. B., Park, Y. Y. (2003). Preparation of water-soluble chitosan/heparin complex and its application as wound healing accelerator. *Biomaterials*, 24, 1595-1601.
17. Lee, M. W., Hung, C. L., Cheng, J. C., Wang,Y. J. (2005). A new anti-adhesion film synthesized from polygalacturonic acid with 1-ethyl-3-(3-dimethylaminopropyl) carbodiimide crosslinker. *Biomaterials*, 28, 3793-3799.
18. Leicht, P., Siim, E., Dreyer, M., Larsen, T. K. (1991). Duoderm application on scalp donor sites in children. *Burns*, 17, 230-232.
19. Li, H., Fu, X., Zhang, L., Huang, Q., Wu, Z., Sun, T. (2008). Research of PDGF-BB gel on the wound healing of diabetic rats and its pharmacodynamics. *Journal of Surgical Research*, 145, 41-48.
20. Macleod, T. M., Williams, G., Sanders, R., Green, C. J. (2005). Histological evaluation of Permacol as a subcutaneous implant over a 20-week period in the rat model. *British Journal of Plastic Surgery*, 58, 518-532.
21. Mao, C., Yuan, J., Mei, H., Zhu, A., Shen, J., Lin, S. (2004). Introduction of photocrosslinkable chitosan to polyethylene film by radiation grafting and its blood compatibility. *Materials Science & Engineering. C, Biomimetic Materials, Sensors and Systems*, 24, 479-485.
22. Monotalbetti, CAGN., Falque, V. (2005). Amide bond formation and peptide coupling. *Tetrahedron*, 61, 10827-10852.
23. Ong, S. Y., Wu, J., Moochhala, S. M., Tan, M. H., Lu, J. (2008). Development of

a chitosan-based wound dressing with improved hemostatic and antimicrobial properties. Biomaterials, 29, 4323-4332.

24. Pollock, T. (1993). Gellan related polysaccharide and the genus Spingomonas. *Journal of General Microbiology*, 139, 1939-1945.
25. Ramires, P. A., Miccoli, M. A., Panzarini, E., Dini, L., Protopapa, C. (2005). In vitro and in vivo biocompatibility evaluation of a polyalkylimide hydrogel for soft tissue augmentation. *Journal of Biomedical Materials Research Part B: Applied Biomaterials*, 72, 230-238.
26. Rinaudo, M. (2004). Role of Substituents on the Properties of Some Polysaccharides. *Biomacromolecules*, 5, 1155-1165.
27. Sen Majumder, P., Bhowmick, A. K. (1999). Surface-and bulk-properties of EPDM rubber modified by electron beam irradiation. *Radiation Physics and Chemistry*, 53, 63–78.
28. Sudhamani, S. R., Prasad, M. S., Udaya, Sankar. K. (2003). DSC and FTIR studies on Gellan and Polyvinyl alcohol (PVA) blend films. *Food Hydrocolloid*, 17, 245-250.
29. Vijayabaskar, V., Tikku, V. K., Bhowmick, Anil K. (2006). Electron beam modification and crosslinking: Influence of nitrile and carboxyl contents and level of unsaturation on structure and properties of nitrile rubber. *Radiation Physics and Chemistry*, 75, 779–792.
30. Wang, C. M., Gong, Y. H., Lin, Y. M., Shen, J. B., and Wang, D. A. (2008). A novel gellan gel-based microcarrier for anchorage-dependent cell delivery. *Acta Materialia*, 4, 1226-1234.
31. Wang, T. W., Sun, J. S., Wu, H. C., Tsuang, Y. H., Wang, W. H., Lin, F. H. (2006). The effect of gelatin–chondroitin sulfate–hyaluronic acid skin substitute on wound healing in SCID mice. *Biomaterials*, 27, 5689-5697.
32. Winter, G. D. (1962). Formation of the scab and the rate of epithelialization of superficial wounds in the skin of the young domestic pig. *Nature*, 193, 293–294.
33. Winter, G. D., Scale, J. T., (1963). Effect of air drying and dressings on the surface of a wound. *Nature*, 197, 91-92.
34. Xu, X., Li, B., Kennedy, J. F., Xie, B. J., Huang, M. (2007). Characterization of konjac glucomannan–gellan gum blend films and their suitability for release of nisin incorporated therein. *Carbohydrate Polymers*, 70, 192-197.
35. Yang, J. M., Yang, S. J., Lin, H. T., Wu, T. H., Chen, H. J. (2008). Chitosan containing PU/Poly(NIPAAm) thermosensitive membrane for wound dressing. *Materials Science & Engineering. C, Biomimetic Materials, Sensors and Systems*, 28, 150-156.
36. Yang, X., Yang, K., Wu, S., Chen, X., Yu, F., Li, J., Ma, M., Zhu, Z. (2010).

Cytotoxicity and wound healing properties of PVA/ws-chitosan/glycerol hydrogels made by irradiation followed by freeze-thawing. *Radiation Physics and Chemistry*, 79, 606-611.

主題五：Gellan Gum Films for Effective Guided Bone Regeneration

Abstract

Guided bone regeneration (GBR) films with bioabsorbable characteristics have been employed for surgical procedures to prevent the growth of scar tissue in the bone graft site. GBR films provide an isolated space over regions with defective tissues and prevent the invasion of fibrous connective tissue into the defect space, and can thus promote bone healing. In this study, we employed Gellan gum (GG) as viable film material and evaluated its potential for GBR applications. Three types of GG films (1%, 1.5%, 2%) were prepared. The tensile strength increased with an increase of film thickness. The 2% and 1.5% GG films were 2.87 and 1.96 times, respectively, the tensile strength of the 1% GG film. However, 1%, 1.5% and 2% GG films were degraded in strength by about 60%, 50% and 20% of initial value, respectively, after 30-day shaking test. Consequently, standardized, transosseous, and critical-sized (cavity of 6 mm) skull defects were made in Sprague-Dawley (SD) rats, and the defective regions were covered with the 2% GG film. After 2 months of recovering, the GG film covered regions showed a clear boundary space between connective tissue and evidenced collagen would not grow into the space of the bone defect. It is concluded that the 2% GG film has great promise for application in GBR in general.

1. Introduction

Guided bone regeneration (GBR) is a current treatment to repair bone defects. GBR film, as a physical barrier device to create a space around the defect, prevent the invasion of fibrous connective tissue into the defect space, and can thus facilitate migration and proliferation of desirable cell populations from adjoining tissue margins and thus promote bone healing [1,2]. Various materials, including nondegradable and degradable polymers have been developed to be GBR films [3]. Degradable GBR films have a benefit of avoiding secondary surgery. However, there are still some problems which must be solved, such as fast degradation and poor mechanical strengths of nature polymers [4,5]. The goal of this study was to develop a new GBR film based on Gellan gum (GG) for clinical use.

Gellan gum is an exopolysaccharide (EPS), also known as polysaccharide S-60, which is a gelling agent produced by a non-pathogenic strain of *Pseudomonas elodea*

ATCC 31461 [6,7]. Natural GG is a linearly electronegative EPS. Its main chain is comprised of four repeating carbohydrates, including two D-glucose, one L-rhamnose, and one D-glucuronic acid. In its natural form, GG has two acyl substituted positions (O-acetate and L-glycerate), which are separately connected to C-6 and C-3 positions of the same glucose molecule. On average, each repeated unit of main chain has 1 glycerate and 0.5 acetates [8]. GG has the ability to form gel in the presence of cations, but the presence of acetyl groups could interfere in ion bonding ability. The average molecular weight of GG is approximately 500 kDa [9].

Currently, GG (a biodegradable and food additive approved by the FDA) is extensively used in food industries, but has rarely been investigated for biomedical applications except for use in drug delivery. Wang et al. [10] used modified GG to cultivate human dermal fibroblasts and human fetal osteoblasts and evidenced GG could be as an innovative material in applications of bone engineering. In addition, GG being an anionic polysaccharide could prevent cell adhesion [11]. Our study is to produce regenerative barrier membrane using GG, taking advantage of the anionic charge of the GG; it will repel the same anionic charge possessed by cell membrane. This material could effectively act as a barrier, inhibiting the growth of fibroblasts at the defective part.

2. Materials and methods

2.1 Preparation of Gellan gum film

Gellan gum of 1 g, 1.5 g and 2 g (Sigma G1910) was dissolved in 100 ml DD water and heated at 85-90°C until it became transparent solution. The concentration of gellan solutions were 1%, 1.5% and 2%. These solutions were poured onto the petri dish (diameter 3.5 cm) and evaporated at 40°C for 2 days to obtain the dry films (denoted as 1% GG film, 1.5% GG film and 2% GG film).

2.2 SEM observation

The surface and cross-sectional microstructures of GG films were examined by scanning electron microscope (SEM). Before SEM observation, all samples were dried, and sputter-coated with gold. By JEOL, JSM-5300, Japan. The thickness of various GG films was measured by an electrical thickness tester (Mitutoyo, MDC-25 SB).

2.3 Water content measurement

The water content of GG film was determined by swelling the film in DD-water at room temperature. The weight of the GG film was determined by blotting the film with filter paper to remove absorbed water on the surface. The water contents of GG

films were calculated as [12]:

Water content (WC) = (Ww-Wd) / Ww (1)

where Ww and Wd are the weights of wet and dry film, respectively. Each WC measurement experiment was repeated 3 times, and measurements expressed as average ± standard deviation (SD).

2.4 Mechanical properties measurement

GG films of 1%, 1.5% and 2% were cut into 1 5-cm2 pieces [13]. The film was hydrated in 0.1 M phosphate buffer, pH 7.4, before being subjected to mechanical testing. The mechanical properties of these GG films were measured and the mechanical parameters were recorded automatically by using the H1-KS testing machine (Tinius Olsen) at crosshead speed of 5 mm/min.

2.5 In vitro degradation test

The degradation study of prepared GG films was conducted in vitro by incubating the film in pH 7.4 of PBS (5 ml), and all samples were incubated on a shaker set at 40 rpm and 37°C. At predetermined time intervals (3 days), the film was taken out of the incubation medium, washed with DD-water and dried, and the weight of this film was measured. Another fresh 5 ml PBS was added into the vial for continuum degradation test, expressed as the accumulated weight losses of the film [14].

2.6 Animals and operation procedure

Sprague-Dawley male rats, fed with commercial food and RO water, were used for the animal study. The rats were anesthetized by transabdominal injection of Zoletil 50 and Rompun mixture (1:2) (0.2 ml/200 g). Following the injection, the skull was shaved and the surfaces at surrounding sides of the skull were exposed via full-thickness incision. A man-made defect (6 mm in diameter) was generated with a dental round burr. Prior to implantation, the film (2% GG film ， 10 10 mm2) was hydrated in physiologic saline to restore its elasticity. In the control group, the bone defect was not covered by any gellan film. The wounds were then carefully sutured. For experimental and control groups, initial healing periods of 4 and 8 weeks were allowed during which the test was repeated 3 times at each time point [15].

2.7 Histological preparation and evaluation

After the healing periods, the rats were sacrificed by injecting an overdose of KCl into the heart. The skull tissue containing bone defects was removed by a large-size dental trephine burr. The specimens of center of defect were fixed in 10% neutral-buffered formalin, decalcified in 10% formic acid, dehydrated in an ascending graded series of

ethanol solutions, and embedded in paraffin. A series of 5- m transverse sections encompassing the entire bone defect specimen were prepared and stained with hematoxylin-eosin and then subjected to light microscopic observation. Additionally, Masson's trichrome stain was also used to observe the formation and distribution of connective tissue on the bone defect (collagen stained blue) [16].

3. Results

3.1 Morphology of GG film

Figure 1 shows SEM images of the surfaces and cross-sections of the various GG films (1%, 1.5% and 2%, respectively). All GG films produced by thermal-induced phase separation demonstrated a dense morphological structure. Moreover, the average thicknesses of 1%, 1.5% and 2% GG films were 0.017 ± 0.003, 0.023 ± 0.003 and 0.034 ± 0.002 mm after measurement by digital micrometer (Mitutoyo). Figure 2 shows SEM images of the surfaces and cross-sections of the 2% GG film after 20 days of shaking. SEM examinations revealed 2% GG film with pore surface after 20 days of shaking and with good integrity, although there were signs of degradation on the surface. The purpose of membrane for GBR was to prevent apical migration of fibroblasts into bony defect site and promote growth of progenitor bone cells. Therefore, dense structure in the initial phase of healing and having pore structure in the later stage was essential for cellular adaptation and sufficient nutrient permeation.

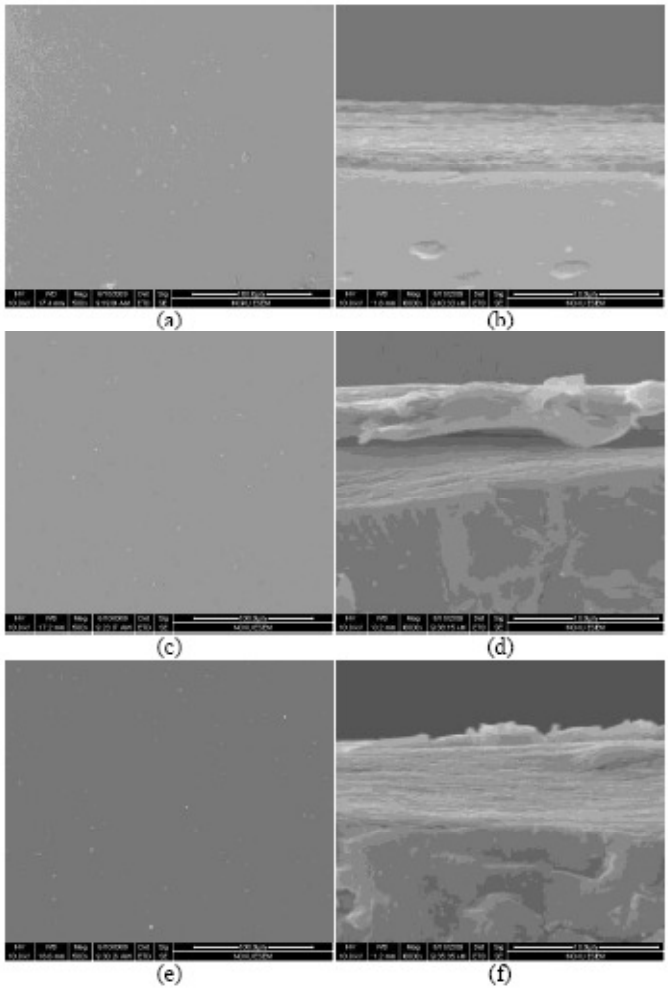

Figure 1. SEM micrographs of the Gellam gum films: (a) surfaces and (b) cross-sections of the 1% GG film; (c) surfaces and (d) cross-sections of the 1.5% GG film; (e) surfaces and (f) cross-sections of the 2% GG film.

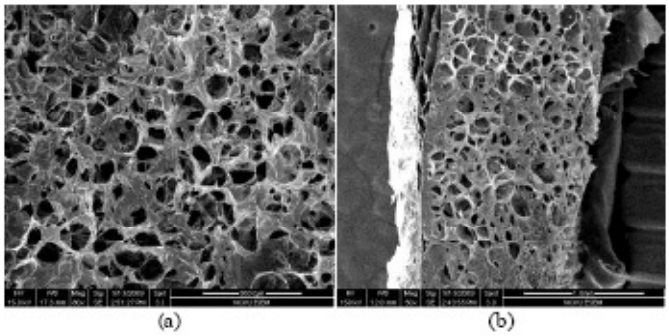

Figure 2. SEM images of the (a) surfaces and (b) cross-sections of the 2% GG film after 20 days of shaking.

3.2 Basic properties of GG film

When considering the development of GBR barrier materials, the basic bulk and mechanical properties must be noted. Additionally, the appropriate degradation rate of materials also has to fit the requirement of tissue regeneration [17]. The mechanical stability of the films was assessed using a tensile test. The maximum load values of a 1%, 1.5%, and 2% GG films are shown in Table 1. The results indicated that tensile strength increases with an increase of film thickness. The 2% and 1.5% GG films were 2.87 times and 1.96 times the tensile strength of the 1% GG film, respectively. In clinical practice, when materials are used as tissue regeneration barrier membranes, they are generally required to maintain certain barrier functions for 4-6 weeks to secure the successful restoration of tissues. As can be seen in Figure 3, 1% GG film was degraded by about 60% of its initial weight after 30-day shaking test. 1.5% and 2% GG films were degraded by about 50% and 20% of initial weight after 30-day shaking test, respectively. From the mechanical property and degradation tests, our results indicated that 2% GG film prepared in this study better fulfilled the requirement for GBR application. Another important characteristic of these GG films was that they could reach steady hydration equilibrium state within the 1 hr period of the experiment, as shown in Figure 4. This rapid swelling phenomenon is beneficial to clinical manageability and surgical procedures.

Table 1. Physical Properties of GG films.

Type of film	Tensile strength, MPa
1.0% GG film	2.32 ± 0.36
1.5% GG film	4.57 ± 0.61
2.0% GG film	6.66 ± 0.31

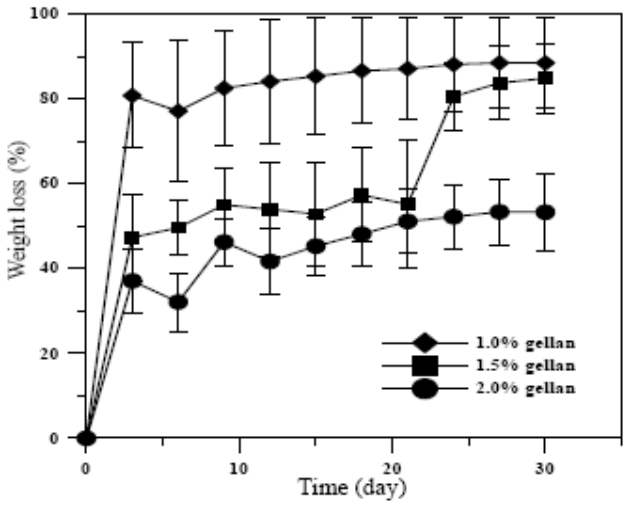

Figure 3. Degradation profile of the membranes in pH 7.4 PBS solution at 37°C for

30-day shaking.

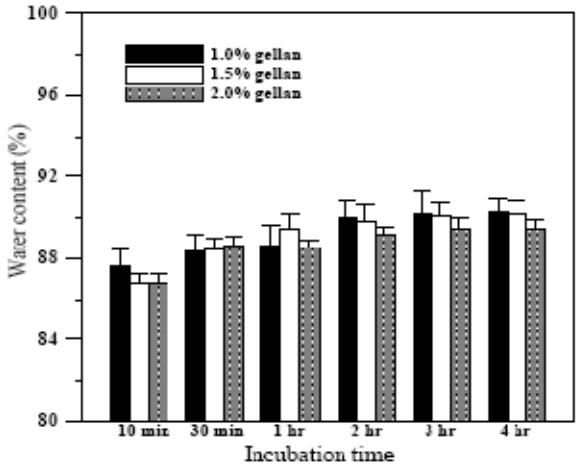

Figure 4. Water content profile of the membranes in pH 7.4 PBS solution.

3.3 Histological observation

Varying degrees of bone healing were observed beneath the 2% GG film in comparison to the control group. In macro vision, for defect covered by 2% GG film two months after surgery, the partially degraded GG film was still visible in the middle of the cut-off portion of the skull (Figure 5(c)). Figures 5(b) and 5(d) show the transverse sections stained by Masson's trichrome of experimental bone defect two months after surgery. In the control, the connective tissue (collagen was stained blue) grew into the bone defect area and prevented the bone cells from growing back to their nature form or space, and thus destroyed the wholesome process of new bone growth. Interestingly, in the experimental group (defect covered with 2% GG film), collagen did not grow into the space of the bone defect. Sequential speaking, the bone defect was allowed with the space and critical healing time to be repaired by newly yet slowly formed bone that proliferated in regions partially or fully protected and separated by the 2% GG film. This process practically prevented any of connective tissue from invading into the bone defect. Furthermore, no obvious inflammatory response was observed around the GG film during initial healing stage. The preliminary results demonstrated that the prepared GG film in this study could successfully isolate the bone defect from ingress of connective tissue cells and provide with the space where bone tissue cells could grow. In addition, the GG films had other advantages, including the easy gel-forming properties, biodegradable and being inexpensive. Full utilization of the characteristics of gellan gum could make it a promising material for GBR application.

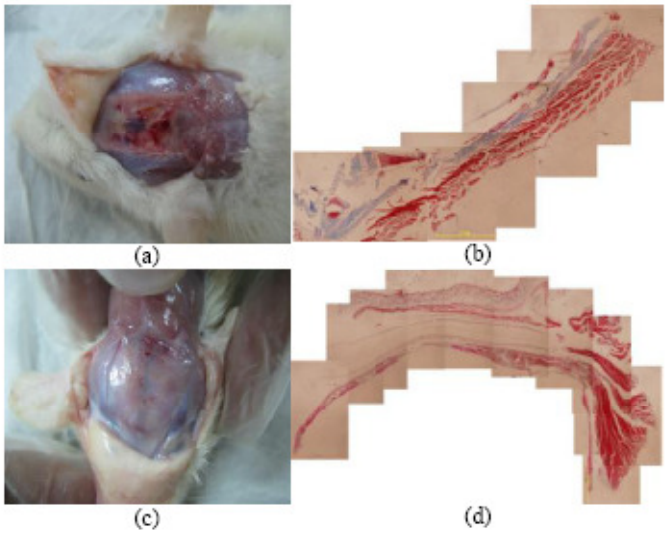

Figure 5. The microscopic appearance of (a) control and (c) GG film observed from an experimental site 2 months after surgery. The transverse sections of (b) control and (d) GG film were stained by Masson's trichrome of experimental bone defect 2 months after surgery.

4. Discussion

Many aspects of technical development of bio-absorbable membrane materials in GBR applications focus on the rigidity and degradation rate, and with special emphasis on the ease of clinical manageability. Lots of effort has been spent on improving the biological function of barrier membrane. For example, surfaces coated with alginate were found to resist cell adhesion [12]. In this study, we studied the microbial polysaccharide gellan gum, which is abundant and inexpensive, and possesses excellent biocompatibility and biodegradable characteristics in applications for GBR. Consequently, we report here in detail a simple phase-induced separation method to prepare 1%, 1.5% and 2% GG films. Briefly, the maximum load value of 2% GG film was 6.6 MPa, about the same mechanical property as chitosan fibrous mesh for application [18]. Following the process, GG films exhibited dense morphological structure that might prevent apical migration of fibroblasts into bony defect sites. We also observed that 2% GG film was not dissolved completely even after 30 days of shaking. Subsequently, we applied 2% GG film to the animal GBR study model. Based on the findings from the histological evaluation, the film exhibited better film integrity in the bone defect healing after 2 months and provided good cell separation ability (see Figs. 5(c-d)) than control (Figs. 5(a-b)). Among the GG films tested, the defect covered with 2% GG film collagen did not grow into the space of the bone defect. On the contrary, in case of the control group, the connective

tissue might have grown preemptively into the bone defect area, and that caused the bony cells, at much slower growth rate, to not be able to grow back into their original space or form. Another important factor for the success of GBR techniques is that the barrier material ought to withstand a period long enough for the bony tissue to reach sufficient healing stage. In clinical practice, tissue regeneration barrier membranes are generally required to maintain their barrier functions for 4-6 weeks to secure the restoration of tissues [12,13]. Our results from Fig. 5(c) showed that 2% GG film was suitable for GBR in biodegradable characteristics. On the basis of the results observed, it could be concluded that the 2% GG film prepared in this study appeared to be of great promise for application in GBR.

References

[1] H. Umeda, S. I. Kanemaru, M. Yamashita, T. Ohno, A. Suehiro, Y Tamura, S. Hirano, T. Nakamura, K. Omori and J. Ito, "In situ tissue engineering of canine skull with guided bone regeneration," *Acta Oto-Laryngol.*, 129: 1509-1518, 2009.

[2] W. J. Cho, J. H. Kim, S. H. Oh, H. H. Nam, J. M. Kim and J. H. Lee, "Hydrophilized polycaprolactone nanofiber mesh- embedded poly (glycolic-co-lactic acid) membrane for effective guided bone regeneration," *J. Biomed. Mater. Res. A*, 91: 400-407, 2009.

[3] S. H. Oh, J. H. Kim, J. M. Kim and J. H. Lee, "Asymmetrically porous PLGA/Pluronic F127 membrane for effective guided bone regeneration," *J. Biomater. Sci.-Polym. Ed.*, 17: 1375- 1387, 2006.

[4] K. Fujihara, M. Kotaki and S. Ramakrishna, "Guided bone regeneration membrane made of polycaprolactone/calcium carbonate composite nano-fibers," *Biomaterials*, 26: 7447-7456, 2005.

[5] H. Maeda, T. Kasuga and L. L. Hench, "Preparation of Poly(l-lactic acid)-polysiloxane-calcium carbonate hybrid membranes for guided bone regeneration," *Biomaterials*, 27: 1216-1222, 2006.

[6] S. K. Kenneth, T. C. George and T. V. George, "Deacetylated polysaccharide S-60," US Patent No. 4326052, 1982.

[7] T. Pollock, "Gellan related polysaccharide and the genus *Sphingomonas*," *J. Gen. Microbiol.*, 139: 1939-1945, 1993.

[8] P. Jansson, B. Lindberg and P. A. Sandford, "Structural studies of gellan gum, an extracelullar polysaccharide elaborated by *Pseudomonas elodea*," *Carbohydr. Res.*, 124: 135-139, 1983.

[9] J. Bemiller, "Structure-property relationships of water-soluble polysaccharides," *J. Appl. Glycosci.*, 43: 377-384, 1996.

[10] C. Wang, Y. Gong, Y. Lin, J. Shen and D. A. Wang, "A novel gellan gel-based

microcarrier for anchorage-dependent cell delivery," *Acta Biomater.*, 4: 1226-1234, 2008.

[11] M. W. Lee, C. L. Hung, J. C. Cheng and Y. J. Wang, "A new anti-adhesion film synthesized from polygalacturonic acid with 1-ethyl-3-(3-dimethylaminopropyl) carbodiimide crosslinker," *Biomaterials*, 26 : 3793-3799, 2005.

[12] T. W. Chen, S. J. Chang, G. C. C. Niu, Y. T. Hsu and S. M. Kuo, "Alginate-coated chitosan membrane for guided tissue regeneration," *J. Appl. Polym. Sci.*, 102: 4528-4534, 2006.

[13] S. M. Kuo, S. J. Chang, G. C. C. Niu, C. W. Lan, T. W. Chen and C. Z. Yang, "Guided tissue regeneration with use of β-TCP/chitosan composite membrane," *J. Appl. Polym. Sci.*, 112: 3127-3134, 2009.

[14] S. V. Fulzele, P. M. Satturwar and A. K. Dorle, "Novel biopolymers as implant matrix for the delivery of ciprofloxacin: biocompatibility, degradation, and *in vitro* antibiotic release," *J. Pharm. Sci*., 96: 132-144, 2007.

[15] S. M. Kuo, S. J. Chang, T. W. Chen and T. C. Kuan, "Guided tissue regeneration for using a chitosan membrane: an experimental study in rats," *J. Biomed. Mater. Res. A*, 76: 408-415, 2006.

[16] R. Liang, S. L. Woo, T. D. Nguyen, P. C. Liu and A. Almarza, "Effects of a bioscaffold on collagen fibrillogenesis in healing medial collateral ligament in rabbits," *J. Orthop. Res*., 26: 1098-1104, 2008.

[17] P. Robert, J. Mauduit, R. M. Frank and M. Vert, "Biocompatibility and resorbability of a polylactic acid membrane for periodontal guided tissue regeneration," *Biomaterials*, 14: 353-358, 1993.

[18] Y. Ku, I. K. Shim, J. Y. Lee, Y. J. Park, S. H. Rhee, S. H. Nam, J. B. Park, C. P. Chung and S. J. Lee, "Chitosan/poly (L-lactic acid) multilayered membrane for guided tissue regeneration," *J. Biomed. Mater. Res. A*, 90: 766-772, 2009.

2012 第九次世界生物材料大會 (9th World Biomaterials Congress, 2012)心得報告

撰寫人: 李明偉 副教授

單位: 中山醫學大學醫學檢驗暨生物技術學系

國科會計劃編號: NSC 98-2221-E-040-007-MY3

一、大會相關資訊

四年一次的世界生物醫學材料會議，於 2012 年已邁入第九屆。第八屆(2008 年)於荷蘭的阿姆斯特丹舉行，第九屆(2012 年)於中國四川的成都舉行，第十屆(2016 年)則是預計於加拿大蒙特羅舉辦。由於此會議是全球從事生物醫學材料相關研究員、廠商四年才舉行一次的國際性會議，每次均吸引將近 3 千位學者專家與會。本次會議的大會主席是中國四川大學的 Xingdong Zhang (張康棟)教授。根據大會提供的資訊，此次會議接受之論文摘要將近 3000 篇，來自於 57 個國家，其中有 75%的論文是出自非地主國地區，近 40%是屬於發展中的國家。顯示生物醫學材料這個領域，目前是處於一個蓬勃發展的階段。

本次會議共安排了一場特別演講、87 場 keynote presentations、976 場口頭論文報告以及 1689 篇壁報論文。另外也安排近 80 家廠商進行生醫產品的展示。會議期間由 6 月 1 日至 5 日。不過會議的第一天是安排開幕和 welcome reception，第二天開始才是正式的學術演講及討論會議。四天當中共有 168 場次(s168)的課程，每一個場次是 2 個小時，同一個時間點有 12 場同步於 12 個會議廳中進行，每一個場次則是安排 7 個口頭論文報告。每一個場次大會均會定義其主題，例如 S001 的主題是 Biomaterials for stem cell control、S036 是 Degradable biopolymers、S079 是 Hybrid materials 等。另外，還有三個 workshop，主題分別是 Tissue inducing biomaterials、Surface characterization、Application of resorbable polymers in medical implant devices。由以上的說明，可以了解此次會議的規模以及內容安排的計劃大綱。

二、與會的過程

吾人參與本次會議，在經費上是由國科會專題研究計劃補助(國科會計劃編號: NSC 98-2221-E-040-007-MY3)。為增加學生的國際視野，此次，並有一名碩士班研究生(中山醫大醫技所黃怡婷同學)隨行。不過，該生並未獲得國科會、教育部以及校方的任何資助，是以自費的方式參加本次的會議。我們於 6 月 1 日搭乘國泰航空 CX465 前往香港，再轉搭港龍航空 KA820 前往成都，抵達成都為當日下午 2 點鐘。回程則是搭乘 6 月 7 日的港龍航空 KA821 抵達香港，再轉搭國泰航空 CX402 回到台灣桃園機場。

本次會議，我們共發表了 5 篇壁報論文，相關資訊如下表所示:

壁報編號	研究主題
P-SAT-C-055	Prevention of tissue adhesion with photocrosslinked gellan gum film
P-SAT-C-263	Gellan gum membrane crosslinked by EDC for preventing postoperative adhesion
P-SAT-B-055	Application of impedance biosensor in diagnosis myocardial injury
P-SAT-A-233	Screen-printed collagen substrate for the biosensor application
P-SAT-A-243	The study of gelatin as an electrode substrate for biosensor system

壁報論文發表，大會安排在 6 月 3 日下午的 17:45—19:45，不過我們在 6 月 2 日當天即將壁報張貼在指定的地點，直到 6 月 4 日早上才將壁報撤下，壁報論文發表之情形如圖 1、圖 2、圖 3 所示。

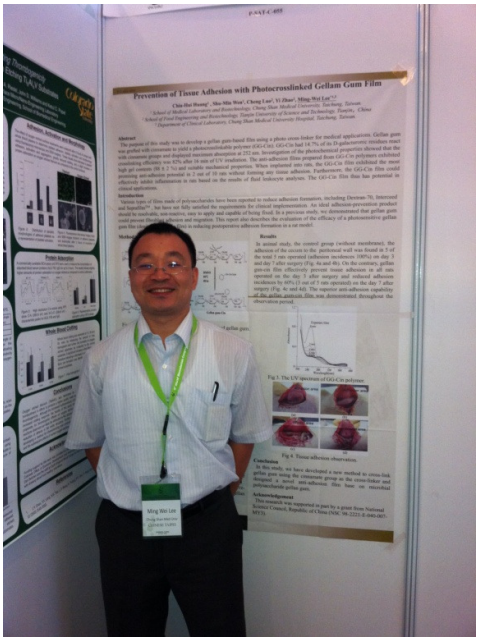

圖 1：壁報展示(P-SAT-C-055)

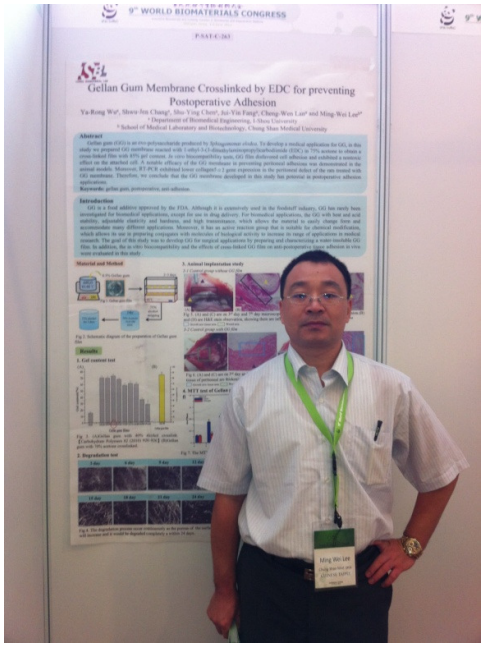

圖 2：壁報展示(P-SAT-C-263)

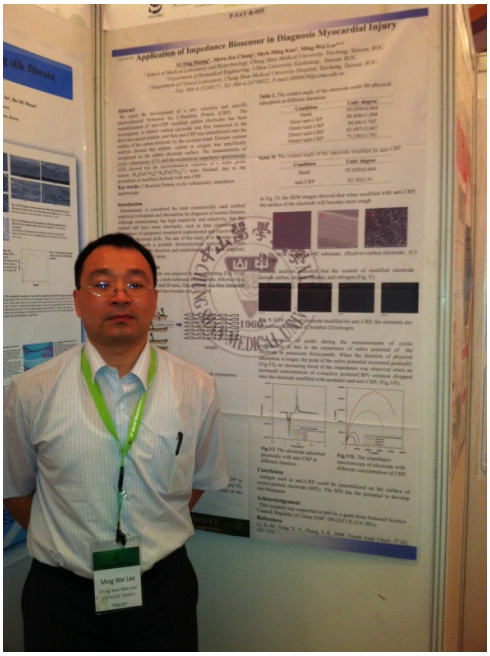

圖 3：壁報展示(P-SAT-B-055)

本次發表的論文，皆是吾人執行國科會專題研究計劃之產出，此計劃的研究主題是關於新型生醫材料 gellan gum 的開發，因此受到相當多研究人員的注意。當

中也有學者提出關於研究構想、材料製備方法、未來應用等問題。由於，很多關於 gellam gum 的研究，本實驗室尚在嘗試階段。因此、對於國外學者所提的問題，我們並沒有很詳細的回答。先前，大會也曾要求我們改以口頭發表，與大家分享研究成果，由於上述的原因，我們還是決定以壁報方式發表。

另外，本次會議我們發表的壁報編號 P-SAT-C-055，已於 2012 年 5 月 2 日寫成完整論文並投稿至 Carbohydrate polymers (IF 3.462， Ranking 3/70)，並於此次會議期間(6 月 5 日)同時收到期刊的審查結果為 minor for acceptance，對於我們是一個很大的鼓舞，也證實了我們的研究成果受到認同，的確有其學術的價值。

三、與會心得

本次會議由於同一時段安排的場次多達 12 個，且與會人員眾多，要聽完每一場的口頭報告，有其時間和空間上的限制。先就每天早上 8-10 點安排兩場的 keynote presentations 來說。主講者皆是生醫材料界資深且研究成果豐碩的著名教授，包括 Nicholas A. Peppas、William Bonfield、Allan S. Hoffman、Kazunori Kataoka 以及 Rocky S. Tuan(旅美台灣人)等人。原本期望這些資深學著能在本會議中提出新的研究方向或是建議。但就演講內容而言，反而多著重在簡介或是概括式的介紹，或許是受限於時間或是與會人員的層次多元，導致較少著墨在研究內容的分享，是吾人感到比較失望的一點。在 oral presentations 方面，吾人參與的場次有 S003(Tissue engineering and regenerative medicine international society)、S018(Surface initiated polymerization for bioactive surfaces)、S026(Cardiovascular tissue engineering)、S042(Immobilization of biological molecules)、S050(Cardiovascular tissue engineering)、S079(Hybrid materials)、S086(Hybrid biomaterials and drug delivery system)、S134(Unique biomaterials for tissue engineering and regenerative medicine)、S148＆S160 (Polymer design for biomedical applications)等。選以上的主題聽講，主要是配合吾人近期的研究方向著重在天

然高分子改質及應用、心肌組織工程、心肌損傷感測技術以及電極表面的生物性分子固定技術等。

在研究內容上，發現大家在研究方法的構思上相差不遠，就心肌組織工程舉例說明，如果真要說差別只是細胞鷹架上的變化而已，甚至看不到新型生醫材料的開發。反倒是在表面改質的議題上，吾人覺得受到比較多的啟發。畢竟化學改質技術是一個比較多變化的領域，學習別人的改質技術再衡量是否可以和自身的研究結合，讓吾人覺得有趣且實用。尤其令我印象深刻的是 Phillip B. Messersmith (USA)的 surface modification 以及 Yoshihiro Sasaki (Japan)的 protein-crosslinked。另外，在組織工程的研究方面，越來越多的研究與臨床結合，這裡所提的臨床指的是已進入人體試驗，特別是日本東京大學的幾個團隊，都有這樣的研究成果。以吾人的了解，關於組織工程產品進入人體試驗在國內的 case 並不多，若以此觀點，似乎本國的進展稍嫌落後。不過，吾人也質疑，人體試驗都必須經過層層嚴格的審查，日本在這方面向來也以學術嚴謹和可信度高著稱，是否這樣的 case 是受到國家專案支持，才得以進行基礎研究與臨床研究的整合，以及大量人力、資源的投入。我們是否應該進一步了解日本的操作模式並考慮效尤，或許是一個重要的關鍵點。

另外，本次會議安排將近 1 千位的口頭報告，但當中有超過半數其實都是在學的學生，且很多不論在英文表達或是問題回答上都不理想。吾人認為在這麼盛大的學術研討會，主辦單位實在有必要控管質與量，否則我們千里迢迢到中國參與該會，卻沒有感受到學術的氛圍，或吸收新的知識，難免會有些遺憾。壁報論文也出現相同的問題，1689 篇論文同時發表，反而讓人感覺不知從何看起。也因為這個問題，導致大會給的會議手冊，只有論文題目，完全沒有論文內容。口頭報告部分也沒有提供任何資訊，當我們對其中某些議題或是結果有疑慮時，完全無書面資料可與研究人員或報告者討論，走馬看花的感覺使得會議淪為形式。很希望能有人跟主辦單位反應此一問題，做為四年後主辦單位的借鏡。

國科會補助計畫衍生研發成果推廣資料表

日期:2012/10/30

國科會補助計畫	計畫名稱: 可降解性Gellan gum做為新型生醫材料之可行性評估		
	計畫主持人: 李明偉		
	計畫編號: 98-2221-E-040-007-MY3　　學門領域: 生醫材料		
研發成果名稱	(中文) 一種傷口敷料及其製造方法		
	(英文) WOUND DRESSING AND METHOD FOR MANUFACTURING THE SAME		
成果歸屬機構	中山醫學大學	發明人(創作人)	李明偉,張淑真,郭士民
技術說明	(中文) 本發明係揭露一種傷口敷料及其製造方法，該傷口敷料係以結蘭膠(Gellan gum)為基材，該結蘭膠係由鞘氨醇單胞菌(Sphingomonas elodea)ATCC 31461 菌株所分泌；此傷口敷料之製造方法係將結蘭膠溶液乾燥形成一結蘭膠薄膜，再利用一交聯劑使結蘭膠薄膜中之結蘭膠分子進行交聯反應，以製成穩定結構之傷口敷料；由於結蘭膠具有生物可降解性，並且以其製備之傷口敷料不具細胞毒性、不會引起血小板吸附、不會引起傷口沾黏、具有促進傷口癒合以及延展性佳等特性，因此以結蘭膠作為基材之傷口敷料係一種非常優良之新穎傷口敷料。		
	(英文) Gellan gum (GG) is an exopolysaccharide produced by Sphingomonas elodea. To develop a medical application for GG, in this study we prepared 26 μm thick films of GG reacted with 1-ethyl-3-(3-dimethylaminopropyl)carbodiimide (EDC) in 40% ethanol to obtain a cross-linked film (GG40) with 73% gel content and 52.4 MPa tensile strength. In vitro biocompatibility tests, GG40 film exhibit nontoxic effects for L929 cells and inhibit absorption and activation of platelets. When implanted into rat subcutaneous tissue, the GG40 film caused minor inflammation in the early postoperative period. The results indicate that the effects of GG40 film on wound healing, wound size reduction (%) and collagen content are higher than those found in commercial products (Duoderm). Therefore, we conclude that the GG film developed in this study has potential for future use in surgical applications.		
產業別	醫療器材製造業		
技術/產品應用範圍	生醫材敷料		
技術移轉可行性及預期效益	技術轉移可行,需廠商協助產品認證		

註：本項研發成果若尚未申請專利，請勿揭露可申請專利之主要內容。

98 年度專題研究計畫研究成果彙整表

計畫主持人：李明偉	計畫編號：98-2221-E-040-007-MY3
計畫名稱：可降解性 Gellan gum 做為新型生醫材料之可行性評估	

成果項目			量化			單位	備註（質化說明：如數個計畫共同成果、成果列為該期刊之封面故事...等）
			實際已達成數（被接受或已發表）	預期總達成數(含實際已達成數)	本計畫實際貢獻百分比		
國內	論文著作	期刊論文	8	6	100%	篇	
		研究報告/技術報告	0	0	100%		
		研討會論文	8	6	100%		
		專書	0	0	100%		
	專利	申請中件數	1	1	100%	件	
		已獲得件數	0	0	100%		
	技術移轉	件數	0	0	100%	件	
		權利金	0	0	100%	千元	
	參與計畫人力（本國籍）	碩士生	2	2	100%	人次	
		博士生	0	0	100%		
		博士後研究員	0	0	100%		
		專任助理	0	0	100%		
國外	論文著作	期刊論文	0	0	100%	篇	
		研究報告/技術報告	0	0	100%		
		研討會論文	0	0	100%		
		專書	0	0	100%	章/本	
	專利	申請中件數	0	0	100%	件	
		已獲得件數	0	0	100%		
	技術移轉	件數	0	0	100%	件	
		權利金	0	0	100%	千元	
	參與計畫人力（外國籍）	碩士生	0	0	100%	人次	
		博士生	0	0	100%		
		博士後研究員	0	0	100%		
		專任助理	0	0	100%		

其他成果 (無法以量化表達之成果如辦理學術活動、獲得獎項、重要國際合作、研究成果國際影響力及其他協助產業技術發展之具體效益事項等，請以文字敘述填列。)	與 University of Tartu Institute of Molecular and Cell Biology()的教授 Cheng Luo 建立合作關係共同開發微生物多醣體之生醫應用

	成果項目	量化	名稱或內容性質簡述
科教處計畫加填項目	測驗工具(含質性與量性)	0	
	課程/模組	0	
	電腦及網路系統或工具	0	
	教材	0	
	舉辦之活動/競賽	0	
	研討會/工作坊	0	
	電子報、網站	0	
	計畫成果推廣之參與（閱聽）人數	0	

國科會補助專題研究計畫成果報告自評表

請就研究內容與原計畫相符程度、達成預期目標情況、研究成果之學術或應用價值（簡要敘述成果所代表之意義、價值、影響或進一步發展之可能性）、是否適合在學術期刊發表或申請專利、主要發現或其他有關價值等，作一綜合評估。

1. 請就研究內容與原計畫相符程度、達成預期目標情況作一綜合評估

■達成目標

□未達成目標（請說明，以 100 字為限）

□實驗失敗

□因故實驗中斷

□其他原因

說明：

2. 研究成果在學術期刊發表或申請專利等情形：

論文：■已發表 □未發表之文稿 □撰寫中 □無

專利：□已獲得 ■申請中 □無

技轉：□已技轉 □洽談中 ■無

其他：(以 100 字為限)

已發表 SCI 期刊 6 篇, 另有 2 篇目前在審查階段, 6 篇 SCI 期刊當中 4 篇領域排名在 5.6%. 申請國內專利一件, 目前於公開階段. 本計畫為三年期, 研究成果質與量超越預期目標. 計畫執行其間參與之大專生與研究生也達 8 位, 對於專業人員的訓練提供很好的機會.

3. 請依學術成就、技術創新、社會影響等方面，評估研究成果之學術或應用價值（簡要敘述成果所代表之意義、價值、影響或進一步發展之可能性）（以 500 字為限）

本計畫是開發微生物多醣體 gellan gum 在生醫上之應用. gellan gum 做為生醫材料, 目前研究並不多. 本計畫開發 gellan gum 做為傷口敷料, 牙科填補材, 術後抗沾黏薄膜, 藥物傳輸基質, 以及做為組織工程細胞鷹架等研究, 具有其研究的新穎性與應用性. 過去三年以 gellan gum 研究發表之 SCI 期刊, 並受到國外研究團隊的注意, 並表達合作的意願, 也因此於 2011 年 11 月受邀到大陸天津科技大學進行演講, 對於國際能見度的提升有很大的幫助. 再者, 本研究希望能引入 gellan gum 做為生醫產品開發的選項之一, 也因此將研究成果申請國內專利, 希望國內廠商將來能與本研究室合作, 共同開發此類產品, 做為本國開發生醫材之特色產業. 對社會的影響方面, 本計畫研究經費全數用於研究開發和人員培訓, 參與之學生人數高達 8 位以上, 以計畫執行同時兼顧專業人才訓練, 可以整合研究與教育資源, 是一種社會資源的合理分配, 且本研究室培養之學生, 也都朝向生醫材發展, 達到學以致用的目標. 未來, 本研究室將持續以 gellan gum 為基材, 更深入研究 gellan gum 與生物體之間的交互作用和影響, 預計將研究的方向調整為基礎與應用並重的性質, 強化研究的深度.